

Exploiting Subsite S1 of Trypsin-Like Serine Proteases for Selectivity: Potent and Selective Inhibitors of Urokinase-Type Plasminogen Activator

Richard L. Mackman,^{*,†} Bradley A. Katz,[‡] J. Guy Breitenbucher,[§] Hon C. Hui,[†] Erik Verner,[†] Christine Luong,[‡] Liang Liu,^{||} and Paul A. Sprengeler^{*,‡}

Departments of Medicinal Chemistry, Structural Biology, and Preclinical Sciences, Axys Pharmaceuticals Inc., 180 Kimball Way, South San Francisco, California 94080

Received June 1, 2001

A nonselective inhibitor of trypsin-like serine proteases, 2-(2-hydroxybiphenyl-3-yl)-1*H*-indole-5-carboxamide (**1**) (Verner, E.; Katz, B. A.; Spencer, J.; Allen, D.; Hataye, J.; Hruzewicz, W.; Hui, H. C.; Kolesnikov, A.; Li, Y.; Luong, C.; Martelli, A.; Radika, K.; Rai, R.; She, M.; Shrader, W.; Sprengeler, P. A.; Trapp, S.; Wang, J.; Young, W. B.; Mackman, R. L. *J. Med. Chem.* **2001**, *44*, 2753–2771) has been optimized through minor structural changes on the S1 binding group to afford remarkably selective and potent inhibitors of urokinase-type plasminogen activator (uPA). The trypsin-like serine proteases¹ that comprise drug targets can be broadly categorized into two subfamilies, those with Ser190 and those with Ala190. A single-atom modification, for example, replacement of hydrogen for chlorine at the 6-position of the 5-amidinoindeole P1 group on **1**, generated up to 6700-fold selectivity toward the Ser190 enzymes and against the Ala190 enzymes. The larger chlorine atom displaces a water molecule (H₂O_{1S1}) that binds near residue 190 in all the complexes of **1**, and related inhibitors, in uPA, thrombin, and trypsin. The water molecule, H₂O_{1S1}, in both the Ser190 or Ala190 enzymes, hydrogen bonds with the amidine N1 nitrogen of the inhibitor. When it is displaced, a reduction in affinity toward the Ala190 enzymes is observed due to the amidine N1 nitrogen of the bound inhibitor being deprived of a key hydrogen-bonding partner. In the Ser190 enzymes the affinity is maintained since the serine hydroxyl oxygen O_γ^{Ser190} compensates for the displaced water molecule. High-resolution crystallography provided evidence for the displacement of the water molecule and validated the design rationale. In summation, a novel and powerful method for engineering selectivity toward Ser190 proteases and against Ala190 proteases without substantially increasing molecular weight is described.

Introduction

The selectivity of small-molecule inhibitors toward a protein or enzyme target is often of crucial importance in the development of therapeutically useful molecules. Engineering high selectivity can be especially challenging when the site of interaction between the inhibitor and the enzyme is within a highly homologous region of a large family of enzymes, such as the catalytic site of trypsin-like serine proteases. Within this family of enzymes there are several important therapeutic targets, for example, urokinase-type plasminogen activator (uPA), which is implicated in tumor progression and metastasis,² and the coagulation enzyme factors Xa, VIIa, and IIa (thrombin). The treatment of the disorders in which these enzymes are involved requires selective inhibitors to reduce the risk of nonspecific *in vivo* toxicities, thereby providing a higher chance of clinical success.³

The serine proteases select their substrates by using a sequence of subsites or specificity pockets denoted S4,

S3, S2, S1, S1', S2', S3', etc. which bind corresponding peptides of the physiological substrate P4–P1, on one side of the scissile bond, and P1'–P4' on the other side.⁴ The trypsin-like serine proteases specifically bind arginine or lysine residues in subsite S1. The remaining pockets around the S1 subsite enable these enzymes to refine their preference for a more specific sequence of peptides and therefore a more defined substrate. Small-molecule inhibitors of these particular enzymes have been traditionally designed along very similar principles, with most of the noncovalent, reversible, small-molecule inhibitors possessing a basic charged moiety, such as an amidine or guanidine, that binds in the S1 subsite, making strong interactions with the conserved Asp189 residue. The very small S1 binding inhibitors that have been reported,^{5–13} for example, **2–4** (Figure 1), rarely generate sufficient potency and selectivity to be therapeutically useful. Consequently, potency and selectivity are often enhanced by elaborating the small inhibitors into larger molecules, designed to occupy neighboring subsites, where the target and relevant antitargets are different. For instance, many of the potent and selective factor Xa inhibitors that have been reported tend to span from the S1 to S4 subsites to achieve sufficient potency and selectivity.^{14–18} A drawback of this design strategy to occupy several subsites is that the final molecules can have higher molecular weights, poorer absorption, distribution, metabolism,

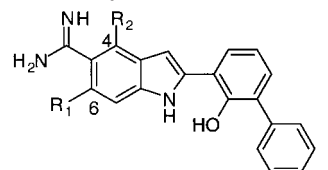
* To whom correspondence should be addressed. (R.L.M.) Phone: (650) 829-1191. Fax: (650) 829-1019. E-mail: richard_mackman@axyspharm.com. (P.A.S.) Phone: (650) 829-1267. Fax: (650) 829-1019. E-mail: paul_sprengeler@axyspharm.com.

[†] Department of Medicinal Chemistry.

[‡] Department of Structural Biology.

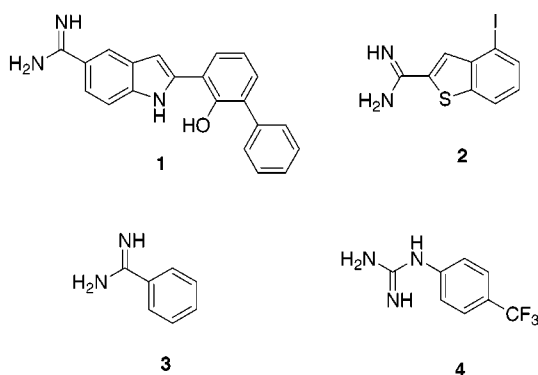
[§] Current address: RW Johnson PRI, 3210 Merryfield Row, San Diego, CA 92121.

^{||} Department of Preclinical Sciences.

Table 1. Effect of Modifications on the P1 Group toward Enzyme Inhibition


compd no.	R ₁	R ₂	formula	K _i (μM)								
				vol ^a	uPA	plasmin	trypsin	FVIIa	FXa	tPA	p-kall.	thrombin
1	H	H	C ₂₁ H ₁₇ N ₃ O	0.0	0.008	0.10	0.13	0.16	0.078	0.035	0.0019	0.32
10a	Cl	H	C ₂₁ H ₁₆ ClN ₃ O	17.5	0.009	0.11	0.23	1.7	19	8.8	0.80	60
10b	F	H	C ₂₁ H ₁₆ FN ₃ O	3.6	0.020	0.35	1.1	0.75	1.3	3.6	0.11	7.5
10c	Me	H	C ₂₂ H ₁₉ N ₃ O	27.2	0.10	0.21	1.6	7.0	>75	39	4.8	>75
10d	OMe	H	C ₂₂ H ₁₉ N ₃ O ₂	35.7	0.36	3.9	14	16	26	18	0.60	>75
10e	OH	H	C ₂₁ H ₁₇ N ₃ O ₂	9.0	2.0	19	50	>75	>75	46	1.3	>75
11	H	Cl	C ₂₁ H ₁₆ ClN ₃ O	17.5	0.49	3.0	4.7	5.5	5.2	3.3	1.3	65

^a Increase in van der Waals volume for H–R₁ compared to H–H. The van der Waals volume of H–R₁ is calculated using the program MOE, and then the volume for H–H, calculated using the same software, is subtracted to estimate the overall increase in van der Waals volume that is created by the substitution R₁.

**Figure 1.** Examples of nonpeptidic small-molecule inhibitors of serine proteases.

and excretion properties (ADME), and often a more challenging synthesis.

Selectivity optimization within subsite S1, a site that is readily accessible and occupied by most, if not all, serine protease inhibitors, could potentially alleviate these drawbacks. Despite the high homologies within this subsite, there are some differences in shape, size, and hydrophobicity that provide each enzyme with a distinct S1 subsite that can be exploited for specificity.^{13,19} For instance, residue 190 is commonly represented as serine, alanine, or threonine within this family of enzymes, the most common targets and antitargets falling into either the Ser190 (uPA, plasmin, trypsin, factor VIIa) or Ala190 (factor Xa, thrombin, plasmin, kallikrein (p-kallikrein), tPA) subclasses. In an earlier paper we describe how a small set of amidine-based S1 binding inhibitors such as **2** and **3** achieve modest selectivity toward the Ser190 enzymes, due, in part, to the formation of an additional hydrogen bond between one of the amidine nitrogens and O_γSer190.¹³ Selectivity can also be observed in small arylguanidine-based S1 inhibitors such as **4**, which have good selectivity toward uPA and against plasmin, tPA, thrombin, and factor Xa.^{12,20,21} Although this selectivity preference toward uPA has eluded satisfactory explanation, it may be due, in part, to the difference in residue 190. Nevertheless, the result remains consistent with the enzymes possessing distinct S1 pockets that provide opportunities for selectivity optimization.

The ability to rationally design inhibitors capable of distinguishing between the Ser190 and Ala190 subclasses of enzymes is a potentially powerful method for generating selective inhibitors between physiologically related enzymes such as uPA (Ser190) and tPA (Ala190) or factor VIIa (Ser190) and factor Xa/thrombin (Ala190). By applying our findings on small S1 amidine-based binding inhibitors that interact with residue 190,¹³ onto a novel, nonselective protease inhibitor, **1**,¹ we have established a method for engineering remarkable selectivity toward Ser190 enzymes and against Ala190 enzymes. A single-atom halogen substitution at the 6-position of the 5-amidinoindole group displaces a hydrogen-bonded water molecule in S1 and produces up to 6700-fold selectivity between these subclasses of enzymes. The design rationale, synthesis, and structural characterization using high-resolution crystallography are presented in this paper. Additionally, the relationship between binding affinity and the increase in the van der Waals size of the group that is introduced is discussed, along with the general application of this novel method for developing selective serine protease inhibitors.

Rationale

The small-molecule inhibitor **1**, previously reported,¹ displays a potency ranging from 2 to 320 nM toward a panel of eight serine proteases (Table 1). High-resolution crystal structures of **1** and related inhibitors²² complexed in uPA (Figures 2a and 3a(i)), trypsin (Figure 3b(i)), and thrombin (Figure 3c(i)) indicate that **1** binds to the catalytic site of the protease and spans from S1 to S1' across the catalytic machinery.¹ Two key sites of interaction between the inhibitor and the enzyme are direct or water-mediated hydrogen bonds to Asp189 and a cluster of short (<2.3 Å) and normal range hydrogen bonds involving the inhibitor, a water molecule (H₂O_{oxy}) trapped in the oxyanion hole, a distally bound water molecule (H₂O_{dis}), and O_γSer195 (Figures 2a and 3a(i)).¹ These interactions with residues that are common to all trypsin-like serine proteases enable **1** to generate high affinity toward many enzymes in the family while maintaining a low molecular weight (327 amu). For example, the affinity toward uPA (K_i = 8 nM, Table 1)

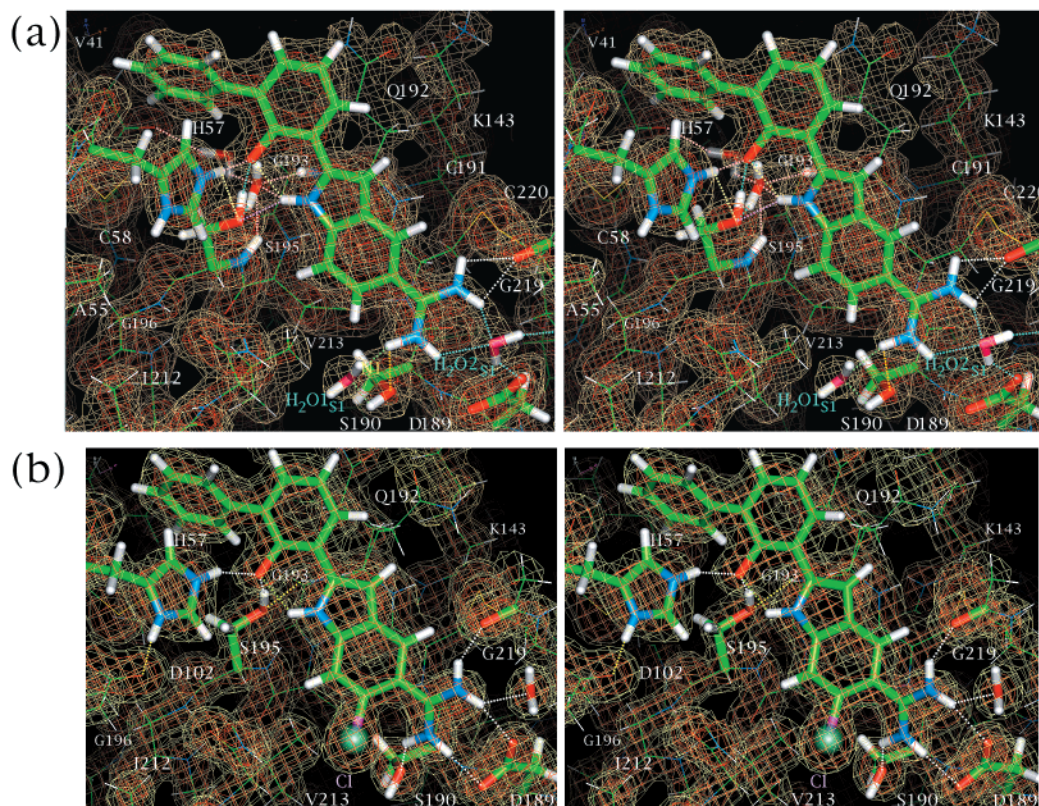


Figure 2. Stereoview X-ray density map of (a) **1** in uPA and (b) **10a** in uPA. In (a) the hydrogen bonds near the catalytic Ser195 are colored as follows: short hydrogen bonds are in cyan, the intra-enzyme and intra-inhibitor in yellow, the other normal range hydrogen bonds in magenta. In S1 the water molecule $\text{H}_2\text{O}_{1\text{S}1}$ is hydrogen bonded to $\text{O}_{\gamma\text{Ser}190}$ and amidine nitrogen N1 (green). Amidine nitrogen N1 also donates a hydrogen bond to $\text{O}_{\gamma\text{Ser}190}$ (yellow). The amidine binds to Asp189 through bridging water molecule $\text{H}_2\text{O}_{2\text{S}1}$. In (b), the density for the chlorine is clearly visible and the amidine N1 makes a full hydrogen bond to $\text{O}_{\gamma\text{Ser}190}$ (white). The inhibitor also makes direct interactions with Asp189. Ser195 moves to occupy the oxyanion hole and is now involved in normal range hydrogen bonds to Gly193 and the inhibitor hydroxyl. This movement of Ser195 has displaced two water molecules that are clearly visible in (a) ($\text{H}_2\text{O}_{\text{oxy}}$ is the nearest water molecule, and $\text{H}_2\text{O}_{\text{dis}}$ is the one furthest back).

is exceptional for a reversible inhibitor of this size and makes **1** an excellent scaffold on which to build selectivity.

To maintain the low molecular weight characteristic of **1**, attention was focused onto the S1 pocket binding motif to improve selectivity. The overall homology and sequence identity for the S1 site region between uPA and several other serine protease enzymes are shown in Figure 4 and Table 2. The highest homology is between uPA and tPA, which is not surprising since they share the same physiological substrate, plasminogen. The homology is much higher (72–89%) when only the residues that contribute to the architecture of the S1 subsite are considered (Table 2). Despite these high homologies within the S1 region, the size and shape of the S1 subsite can differ even when the residues are almost identical.¹³ For example, the depth of the uPA S1 pocket along the Ser195–Asp189 axis is much greater than that of trypsin notwithstanding the high similarity (94%, Table 2). Two of the residues that contribute to the homology variations in the S1 subsite between uPA and the other enzymes are residues 190 and 213. In general, the trypsin-like serine proteases can be divided into four subclasses on the basis of the identity of residue 190: Ser190, Ala190, Thr190, and other residues. All the common targets and antitargets, mentioned herein, fall into either the Ser190 or Ala190 category (Table 2). The 190 and 213 residues both flank a tightly bound water molecule, $\text{H}_2\text{O}_{1\text{S}1}$, that is cobound

with the inhibitor **1** (Figures 2a and 5). It was reasoned that a group introduced at the 6-position of the inhibitor, such as a chlorine, designed to displace $\text{H}_2\text{O}_{1\text{S}1}$ (Figure 5), could impart selectivity since the residues that flank $\text{H}_2\text{O}_{1\text{S}1}$ are different between closely related targets and antitargets, e.g., uPA and tPA. Displacement of a tightly bound water molecule can also be expected to provide an entropic advantage toward binding.²³ Furthermore, the crystal structures of the Ser190 enzymes bound by **1** (Figures 2a and Figure 3a–c(i)) indicate that the amidine nitrogen N1 has partial hydrogen bonds to the cobound water ($\text{H}_2\text{O}_{1\text{S}1}$) and $\text{O}_{\gamma\text{Ser}190}$, but, in contrast, the Ala190 enzymes accommodate the lack of $\text{O}_{\gamma\text{Ser}190}$ by the formation of a full hydrogen bond between the amidine nitrogen N1 and $\text{H}_2\text{O}_{1\text{S}1}$. This subtle difference in hydrogen bond length emphasizes the importance of the water molecule toward binding in the Ala190 enzymes. The 6-chloro-substituted analogue of **1** and also other 6-substituted 5-amidinoindoles were therefore targeted to test this hypothesis.

Chemistry

The synthesis of **1**, described earlier,¹ involved the use of the Fisher indolization procedure.²⁴ Applying the same strategy to the synthesis of the desired 2,5,6-trisubstituted indoles yielded a mixture of regioisomers, due to the asymmetric nature of the hydrazone intermediate **9** (Scheme 1). For example, the condensation of acetophenone **8** with hydrazine **7** to give the asym-

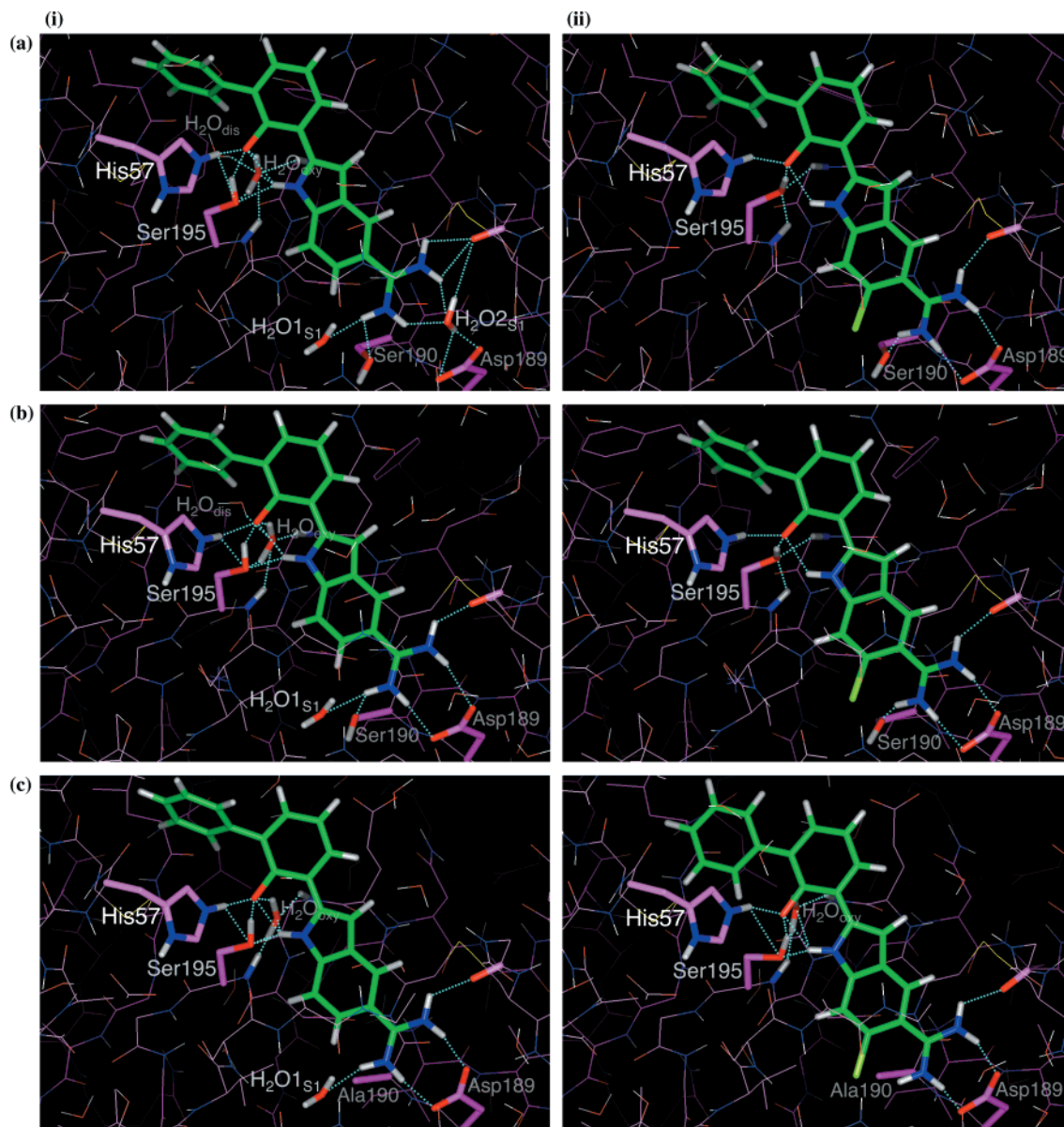


Figure 3. Side by side binding in (a) uPA, (b) trypsin, and (c) thrombin (modeled from the isosteric benzimidazole version of **1** in thrombin³²) of **1** (i) and **10a** (ii). In (a)(ii), (b)(ii), and (c)(ii) note the loss of H₂O_{1s1} in all the **10a** complexes and also the tilt of the inhibitor **10a** compared to **1**. In (a) note that three more water molecules are displaced. Ser195 moves into the oxyanion hole and displaces H₂O_{oxy} and H₂O_{dis}. Asp189 moves to make direct interactions with the amidine, thus displacing H₂O_{2s1}. In (b) Ser195 moves into the oxyanion hole similar to (a) and displaces H₂O_{oxy} and H₂O_{dis}. In (c) the complex of **1** is modeled on the basis of the complex of the isosteric benzimidazole version of **1** in thrombin.³² Only one water molecule is displaced, notably H₂O_{1s1}. Ser195 does not move, and H₂O_{oxy} and H₂O_{dis} are not displaced.

metric hydrazone **9**, followed by polyphosphoric acid (PPA) mediated Fisher indolization, resulted in an equimolar mixture of 6-chloro-2-(2-hydroxybiphenyl-3-yl)-1*H*-indole-5-carboxamide (**10a**) and 4-chloro-2-(2-hydroxybiphenyl-3-yl)-1*H*-indole-5-carboxamide (**11**) (1:1 ratio determined by HPLC methods). These isomers could only be separated by careful preparative HPLC, resulting in a substantial loss of material, thus prompting the investigation of an alternative, more regioselective method for the synthesis of 2,5,6-trisubstituted indoles. Buchwald and co-workers found that milder Fisher indolization conditions can afford good regiocontrol of the indolization step following hydrazone formation.²⁵ Unfortunately the milder conditions do not effect cyclization when electron-withdrawing groups such as amidine and chlorine are present. Substituted 2-arylin-

doles have been readily prepared using a palladium-catalyzed coupling of an alkyne onto an *o*-iodoaniline followed by cyclization of the resultant 2-ethynylaniline to the indole heterocycle.^{26–30} For example, Yasuhara et al. produced a variety of 2,5-substituted and 2,6-substituted analogues very efficiently and in good yield using this methodology.²⁶ Furthermore, the conditions appear to be compatible with many different functional groups including halides and nitriles, which can be readily transformed into amidines. The control of regioselectivity is provided by the substitution pattern on the aryl halide, which can be easily controlled through the selective synthesis of *o*-iodoanilines. A retrosynthetic scheme in which the 6-substituent can be varied is shown in Scheme 2. Synthesis would require a common

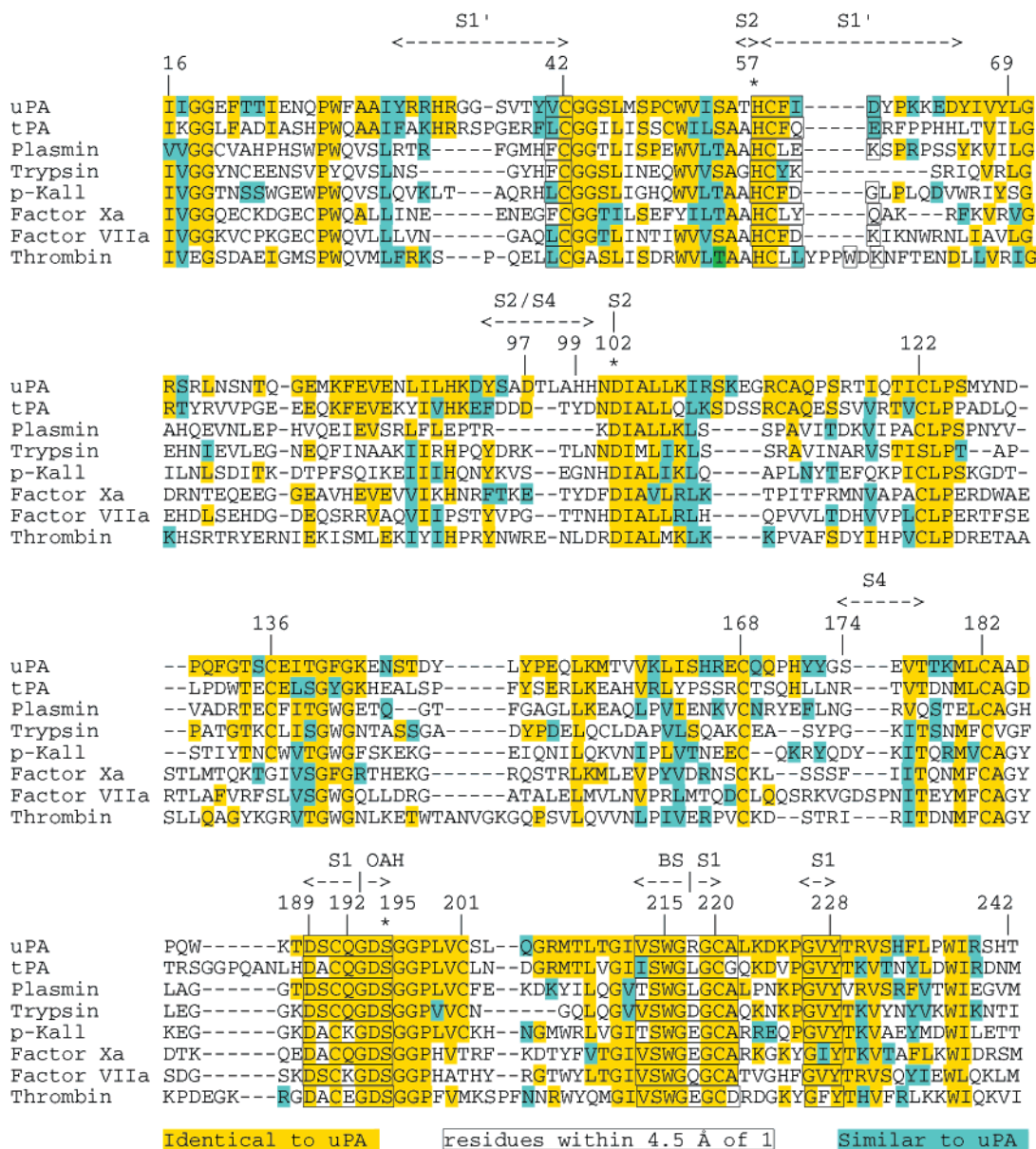


Figure 4. Sequence homology among several trypsin-like serine proteases compared to uPA. The chymotrypsin numbering system was used throughout. OAH = oxyanion hole, and BS = β strand. Residues of the catalytic triad are marked by an asterisk.

Table 2. Homology Comparisons between uPA and Related Enzymes

	entire sequence of residues (%)		residues within 4.5 Å of 1 ^b (%)		S1 subsite residues ^c (%)		residue 190
	identical	similar ^a	identical	similar	identical	similar	
tPA	45	54	72	84	78	83	alanine
plasmin	37	48	76	76	89	89	serine
trypsin	37	47	76	80	89	94	serine
p-kallikrein	33	45	72	76	78	78	alanine
factor Xa	30	43	72	76	83	89	alanine
factor VIIa	30	39	80	84	89	89	serine
thrombin	25	36	64	72	72	72	alanine

^a Residues were considered similar only if they had both similar charge/hydrophobicity and size. ^b Twenty-five residues were included in the comparison (see the boxed residues in Figure 4). ^c The 18 residues used for comparison are 189–195, 213–220, and 226–228.

phenylacetylene component, **13**, and a variety of 2-substituted 4-amino-5-iodobenzonitriles, **12**.

The MEM-protected phenol **13** has been previously synthesized.¹ The precursors **12a–e** were obtained according to Schemes 3–6. The 2-halogen-substituted 4-amino-5-iodobenzonitriles **12a** and **12b** were prepared according to procedures outlined in Scheme 3. The

methyl group of nitrotoluene **15** was oxidized to acid **16** and then transformed to the nitrile **17** via the amide, in a yield of 29% from **15**. Reduction of the nitro group then afforded the aniline **18** in high yield. Commercial aniline **5** and aniline **18** were both converted to aryl halides **12a** and **12b** in yields of 48% and 33%, respectively, using *N*-iodosuccinimide (NIS) in acetic acid.

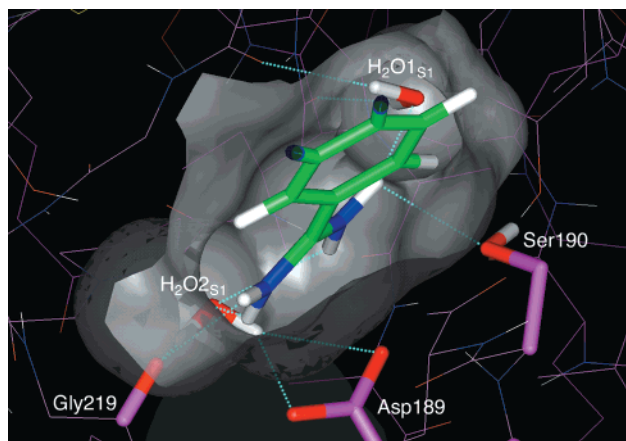
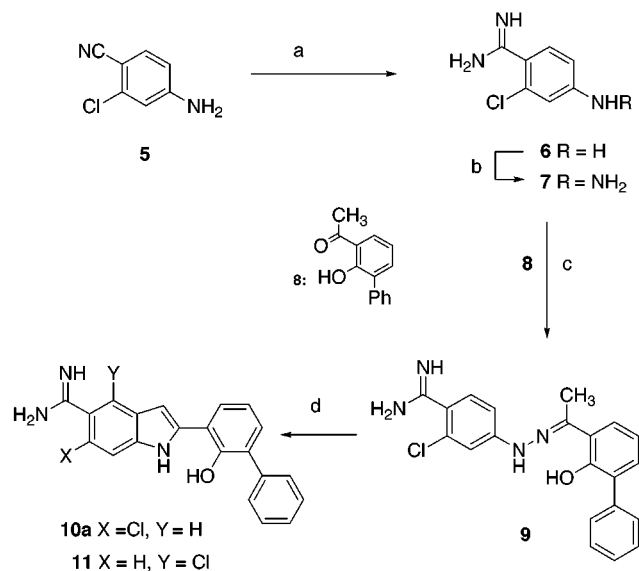


Figure 5. Close-up view of the base of the S1 subsite in the uPA-1 complex. $\text{H}_2\text{O}_{1\text{S}1}$ is situated in a small pocket in the upper right which can be accessed most readily from the 6-position of the heterocyclic ring. The size of the small pocket occupied by $\text{H}_2\text{O}_{1\text{S}1}$ is close to the van der Waals volume of chlorine.

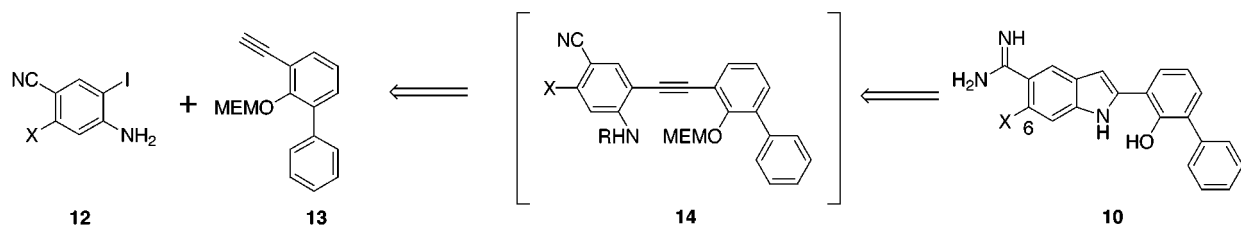
Scheme 1^a



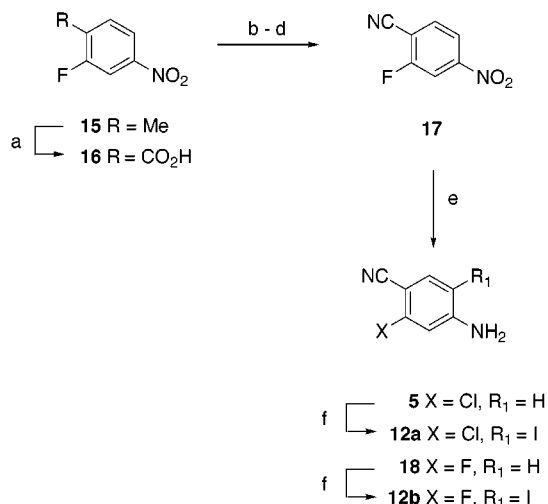
^a Reagents and conditions: (a) Me_3Al , NH_4Cl , *p*-xylene, reflux; (b) NaNO_2 , 6 N HCl, 0 °C, then $\text{SnCl}_2 \cdot 2\text{H}_2\text{O}$; (c) **8**,¹ EtOH, Et_3N , reflux; (d) PPA, 155 °C.

Aniline **19** was transformed into benzonitrile **20** in 91% yield through cyanide displacement of the diazonium salt (Scheme 4). Tin(II) chloride reduction of **20** afforded aniline **21**, which was then converted to 4-amino-5-iodo-2-methylbenzonitrile (**12c**) in 53% overall yield using NIS in acetic acid. To prepare **12d**, the 1,2-methylene-dioxy ring of **22** was opened using sodium cyanide in HMPA,³¹ and treatment of the phenol **23** with methyl iodide gave methyl ether **24**, in 28% yield over two steps

Scheme 2. Proposed Regiospecific Synthesis of 6-Substituted 5-Amidino-2-arylimidoles

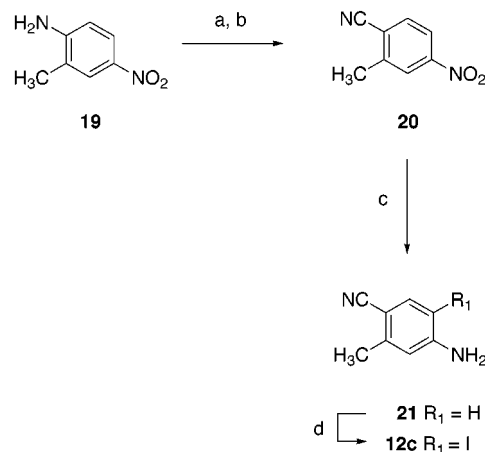


Scheme 3^a



^a Reagents and conditions: (a) CrO_3 , 18 N H_2SO_4 , AcOH, 100 °C; (b) $(\text{COCl})_2$, THF, DMF; (c) $\text{NH}_3(\text{g})$, THF, 0 °C; (d) TFAA, THF; (e) H_2 , 10% Pd/C, MeOH; (f) NIS, AcOH.

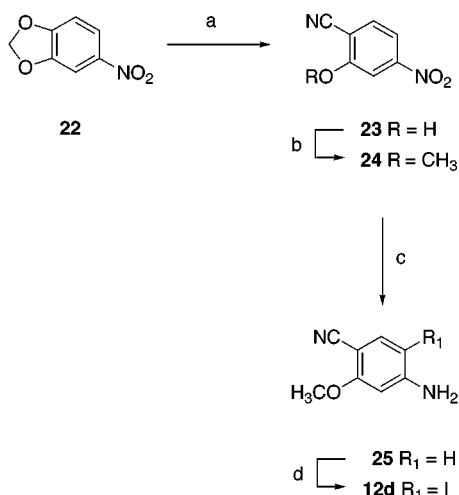
Scheme 4^a



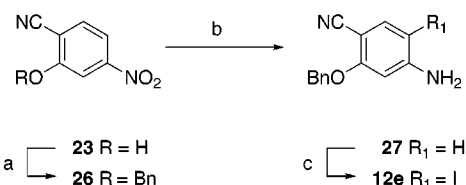
^a Reactions and conditions: (a) NaNO_2 , 18 N H_2SO_4 , AcOH; (b) CuSO_4 , KCN, H_2O , benzene, NaHCO_3 ; (c) $\text{SnCl}_2 \cdot 2\text{H}_2\text{O}$, dioxane, 12 N HCl; (d) NIS, AcOH.

(Scheme 5). Reduction of the nitro group afforded the aniline **25**, which was then treated with NIS to give the desired product **12d**, in 29% yield. Alternatively, the phenol **23** could be converted to benzyl ether **26** and then reduced to provide aniline **27** in a high overall yield (Scheme 6). Subsequent treatment with NIS then afforded 4-amino-5-iodo-2-(benzyloxy)benzonitrile (**12e**) in 80% yield.

A variety of *N*-substituted anilines such as carbamates and mesylates have been used in the palladium-mediated coupling of the alkyne onto the aryl halide (Scheme 7). The work of Yasuhara et al.²⁶ indicated that

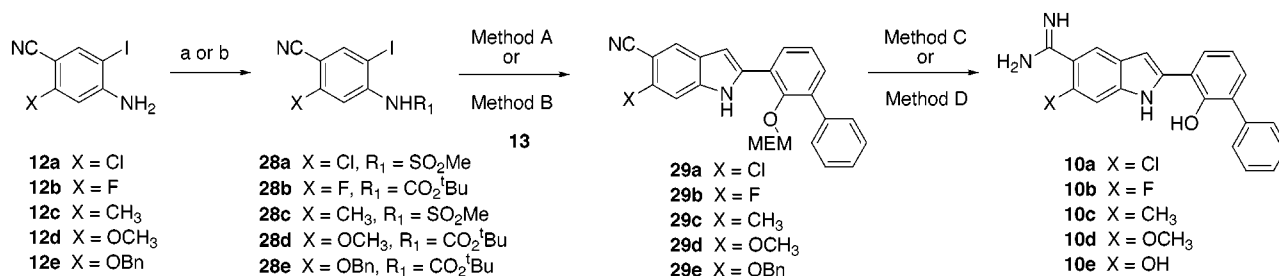
Scheme 5^a

^a Reagents and conditions: (a) HMPA, NaCN, 150 °C; (b) DMF, CH₃I, K₂CO₃; (c) SnCl₂·2H₂O, dioxane, 6 N HCl, 0 °C; (d) NIS, AcOH.

Scheme 6^a

^a Reagents and conditions: (a) BnBr, DMF, K₂CO₃; (b) SnCl₂·2H₂O, dioxane, 6 N HCl; (d) NIS, CH₃CN.

both BOC- and mesyl-substituted anilines can afford 2-aryloindoles in high yields. The benzonitriles **12a–e** were therefore converted into either the mesyl- or BOC-substituted anilines **28a–e** in yields ranging from 42% to 64% (Scheme 7). The palladium(II)-mediated coupling of the alkyne with the mesyl-substituted anilines **28a** and **28c** generated intermediate alkynes which cyclized in situ to the respective *N*-mesylindoles. Removal of the mesyl groups by treatment with sodium hydroxide

Scheme 7^a

^a Reagents and conditions: (a) MsCl, DIEA, CH₂Cl₂, DMAP; (b) di-*tert*-butyl dicarbonate, DIEA, THF or DMF, then 50% NaOH; (method A) DMF, Pd(PPh₃)₂Cl₂, Et₃N, CuI, **13**; then NaOH; (method B) DMF, Pd(PPh₃)₂Cl₂, Et₃N, CuI, **13**; then TBAF; (method C) 50% NH₂OH(aq), EtOH, reflux; then Ac₂O, AcOH; then H₂, 10% Pd/C; then 4 N HCl, dioxane, MeOH; (method D) 50% NH₂OH(aq), EtOH, reflux; then Ac₂O, AcOH.

Table 3. Formation of Indoles Using Palladium-Mediated Coupling of Alkynes with Aryl Halides

aniline	R ₁	X	method	product	yield (%)	method	product	X	yield (%)
28a	SO ₂ Me	Cl	A	29a	52	C	10a	Cl	20
28b	CO ₂ ^t Bu	F	B	29b	44	C	10b	F	20
28c	SO ₂ Me	Me	A	29c	26	C	10c	Me	9
28d	CO ₂ ^t Bu	OMe	B	29d	69	C	10d	OMe	58
28e	CO ₂ ^t Bu	OBn	B	29e	54	D	10e	OH	27

yielded indoles **29a** and **29c** in yields of 52% and 26%, respectively (Table 3, method A). The same palladium(II)-mediated coupling reaction employing the BOC derivatives **28b**, **28d**, and **28e** initially gave the coupled biarylalkyne intermediate prior to formation of the indole heterocycle.²⁶ These intermediates were then treated with TBAF³⁰ to induce cyclization and simultaneous removal of the BOC group, resulting in good yields (>44%) of indoles **29b**, **29d**, and **29e** (method B). In the examples shown in Table 3, the BOC-substituted anilines were generally easier to prepare and tended to give better overall yields of the final products. The conversion of the nitrile groups to amidines was performed using two general procedures (methods C and D) involving hydroxylamine addition, acetylation of the hydroxyamidine, and reduction. The difference between the two procedures was the use of 10% palladium on carbon catalyst rather than zinc dust for the simultaneous reduction of the acetoxyamidine intermediate and the benzyl group in the preparation of the hydroxyl analogue **10e**. In all examples the final step was clean and efficient removal of the MEM protecting group by treatment with hydrochloric acid to yield indoles **10a–e**. On the basis of the results obtained (Table 3), the route has general applicability toward the efficient synthesis of a variety of 2,5,6-trisubstituted indoles.

Results and Discussion

The analogues **10a–e** and **11** were tested for activity toward a panel of eight human serine proteases (Table 1). The enzymes represent a cross section of targets and antitargets from the coagulation cascade and the uPA system, and also the Ala190 and Ser190 subclasses of enzymes. Compared to **1**, the incorporation of a chlorine atom adjacent to the amidine, **10a**, only marginally changed the affinity toward the Ser190 enzymes uPA, plasmin, trypsin, and factor VIIa (all <11-fold), but toward the Ala190 enzymes factor Xa, p-kallikrein, thrombin, and, importantly, tPA, the affinity was dramatically reduced by 244-, 421-, 188-, and 251-fold, respectively. The magnitude of these changes in binding affinity creates a “switchlike” effect whereby the chlo-

rine atom essentially turns "off" (or significantly reduces) the inhibitory activity of **10a** toward all the Ala190 proteases. The single-atom change has therefore produced a highly potent, low molecular weight, selective inhibitor of uPA, with between 90- and 6700-fold selectivity against the Ala190 proteases, and between 12- and 200-fold selectivity against the other Ser190 proteases. The 4-position chlorine analogue **11** had reduced affinity toward all the enzymes including uPA. It is worth noting that **1** is a 2-fold less effective inhibitor of the Ser190 protease factor VIIa, compared to Ala190 protease factor Xa, but the chlorine analogue **10a** is a 10-fold better inhibitor of factor VIIa compared to factor Xa. This moderate 20-fold effect may be of importance in the development of potent and selective factor VIIa inhibitors.

Comparisons between the Binding Modes of Inhibitors 10a and 1. The complexes of **10a** in the Ser190 enzymes uPA and trypsin and Ala190 enzyme thrombin were determined by X-ray methods and compared to the uPA and trypsin complexes of **1**, and a model of the thrombin-**1** complex. The thrombin-**1** complex has not been solved, so the complex of the isosteric 5-amidinobenzimidazole analogue of **1** was used to model the thrombin-**1** complex.³² Earlier results comparing benzimidazole- and indole-based S1 binding groups¹ indicate that the binding modes of inhibitors in which only this group is changed are essentially identical. The interactions in the uPA-**10a** complex (Figures 2b and 3a(ii)) differ quite significantly from those in the uPA-**1** complex (Figures 2a and 3a(i)). In the uPA-**1** complex two water molecules are cobound in S1, the water molecule targeted for displacement, H₂O_{S1}, and a second water molecule, H₂O_{2S1}, that is recruited to bridge the interaction between the amidine group of the inhibitor and Asp189. This second water molecule is only found in the uPA-**1** complex since the S1 subsite of uPA is deeper than that of trypsin and thrombin. The inhibitor is prevented from moving deeper into the S1 pocket to form a direct interaction with Asp189 by the unique cluster of short and normal range hydrogen bonds between the inhibitor and Ser195.^{1,22} In the uPA-**10a** complex, both of the water molecules cobound in S1 are displaced, leaving one full hydrogen bond between the amidine nitrogen N1 and O_γSer190. This is in contrast to the two longer range hydrogen bonds that exist in the uPA-**1** complex between N1 and H₂O_{S1} and O_γSer190. Rather unexpectedly, the short hydrogen bond network outside S1 is sacrificed to allow the inhibitor to bind 0.8–1.0 Å deeper into the S1 pocket. Residue Asp189 shifts 0.5 Å toward the inhibitor to form direct interactions with the amidine, thereby displacing H₂O_{2S1} (Figures 2b and 3a(ii)). The breakdown of the short hydrogen bond cluster outside S1 is also accompanied by the movement of Ser195 to occupy the oxyanion hole, thus displacing H₂O_{oxy} and also H₂O_{dis}. The short hydrogen bond that existed between the inhibitor phenolate and O_γSer195 in the uPA-**1** complex is now an ordinary length (2.60 Å) hydrogen bond in the uPA-**10a** complex. In summation, a total of four ordered water molecules are displaced, while the protein experiences significant shifts of two key residues, Asp189 and Ser195, leading to a breakdown of the short hydrogen bond cluster. Despite these

structural changes, the entropy gain of displacing four water molecules offsets any unfavorable effects on potency and results in a highly potent inhibitor toward uPA (Table 1).

In the thrombin-**10a** complex model (Figure 3c(ii)), the water molecule H₂O_{S1} that is cobound in the complexes of thrombin with two related inhibitors and therefore presumed to be present in the binding of **1** to thrombin^{1,32} is displaced, leaving the amidine without an important hydrogen bond partner. In contrast to the uPA-**10a** complex, the water molecules H₂O_{oxy} and H₂O_{dis} are not displaced in the thrombin-**10a** complex model, and the short hydrogen bonds between the inhibitor hydroxyl, O_γSer195, and H₂O_{oxy} remain intact. Therefore, in thrombin only one water molecule is displaced by **10a**, compared to **1** (Figure 3c(i)), and no major structural changes occur in the position of residues Asp189 and Ser195.

The complex of **10a** in trypsin also confirms that the H₂O_{S1} water molecule has been displaced (Figure 3b(ii)). Similar to the uPA-**10a** complex, H₂O_{oxy} and H₂O_{dis} are also displaced, resulting in the absence of a total of three water molecules. The complex of **1** in trypsin displays direct interactions between the amidine and the Asp189 due to its shallower S1 subsite relative to that of uPA. All three complexes involving **10a** therefore confirm the displacement of H₂O_{S1} as intended in the design of the inhibitor.

The combined structural information clearly reveals the basis for the selectivity enhancements that are observed in the enzyme assays. In the Ser190 proteases the loss of H₂O_{S1} is accompanied by the formation of a full hydrogen bond between nitrogen N1 and O_γSer190. In contrast, inhibitors that displace H₂O_{S1} in the Ala190 enzymes such as thrombin leave the amidine in an environment devoid of both the water molecule and O_γSer190 as hydrogen-bonding partners (Figure 6). This unfavorable situation is manifested in significantly reduced affinities toward the Ala190 enzymes, and hence selective inhibition toward the Ser190 enzymes is generated. Although X-ray structures are not available for all the Ala190 enzymes, it is highly likely that the water molecule is displaced in tPA, factor Xa, and p-kallikrein. Therefore, the displacement of H₂O_{S1} by the appropriate chemical modification of the indole ring is a powerful way of tuning the selectivity of amidine-based protease inhibitors toward Ser190 enzymes and against Ala190 enzymes.

Relationship of Substituent Size toward Inhibitor Binding. All the proteases have an S1 subsite that is subtly different in size and shape. It has already been noted that the S1 subsites of uPA and trypsin have different sizes upon inhibitor binding, despite both enzymes having similar residues lining the S1 pocket (Table 2).¹³ Furthermore, the movement of residue 189, in the case of the uPA-**10a** complex, also implies that there is some flexibility in the position of the S1 subsite residues, which will affect the overall size of the inhibitor bound S1 pocket. The introduction of groups both smaller (fluorine, hydroxyl) and larger (methyl, methoxy) than chlorine provides a method for probing the relationship between the size of the P1 group on the inhibitor and binding affinity. The chemistry scheme, used to prepare **10a**, was easily modified to introduce

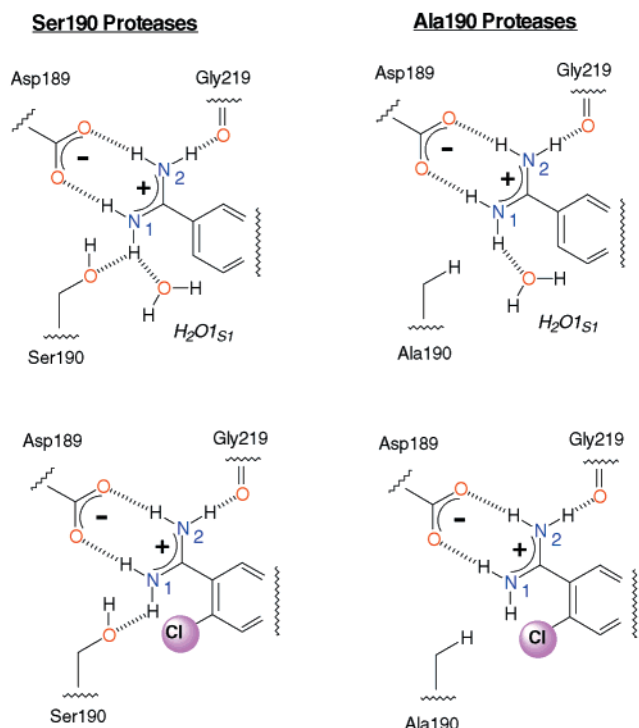


Figure 6. Schematic displaying the basis for selectivity enhancement based on the binding of **10a** in trypsin and thrombin. The typical binding of a 6-unsubstituted amidine, e.g., **1**, to a Ser190 protease such as trypsin is shown in the upper left panel. The amidine N1 atom (blue) has hydrogen bonds to both H_2O_{1S1} and O_{Ser190} (red). The upper right panel shows the typical binding of **1** to an Ala190 protease such as thrombin in which the amidine nitrogen N1 has only one hydrogen bond to H_2O_{1S1} . The lower panels show the situation in which the 6-chlorine substituted analogue **10a** displaces H_2O_{1S1} in both the Ser190 (lower left) and Ala190 enzymes (lower right). In the lower left panel the binding of the 6-chlorine analogue **10a** displaces H_2O_{1S1} and forms one (full) hydrogen bond to O_{Ser190} . In the lower right panel the binding of the 6-chlorine analogue **10a** to the Ala190 proteases leaves the amidine N1 without a full complement of hydrogen-bonding partners, just the Asp189. The hydrogen bond from amidine nitrogen N1 to the Asp189 oxygen remains in all cases.

several different groups at the 6-position (see the Chemistry section).

The smaller fluorine analogue **10b**, compared to the chlorine analogue **10a**, had approximately the same affinity toward all the Ser190 proteases. The affinity

toward the Ala190 proteases was reduced by margins of 17-fold (factor Xa), 103-fold (tPA), 116-fold (p-kallikrein), and 23-fold (thrombin). Although not as impressive as the results with the chlorine analogue, these differences still produce a molecule with selectivities ranging from 6- to 441-fold against all the other enzymes while maintaining a high potency toward uPA ($K_i = 20$ nM). The uPA-**10b** complex is markedly different from the uPA-**10a** complex as a result of the reduced size of the fluorine group (Figure 7). Neither of the two water molecules cobound in subsite S1, H_2O_{oxy} nor H_2O_{dis} , is displaced. The mode of binding in the uPA-**10b** complex is therefore very similar to that of the uPA-**1** complex. This is in stark contrast to the trypsin-**10b** complex in which the fluorine does displace the water molecule H_2O_{1S1} .³² The difference between the uPA and trypsin structures regarding the inclusion or exclusion of H_2O_{1S1} is a reflection of the greater depth of the uPA pocket compared to trypsin, which allows uPA to accommodate both the fluorine and water simultaneously. It is presumed that, in the thrombin-**10b** complex, the water molecule H_2O_{1S1} would also be absent. Therefore, in uPA, which has the deepest and largest S1 subsite, the transition between the H_2O_{1S1} cobound and unbound states occurs upon changing from fluorine to chlorine. This transition occurs upon moving from hydrogen to fluorine in trypsin and, most likely, thrombin. Since selectivity is enhanced in the fluorine analogue **10b**, even though H_2O_{1S1} remains in uPA, it follows that it is only necessary to displace the water molecule from the Ala190 enzymes and not the Ser190 enzymes to achieve the desired selectivity effect.

Investigation of larger groups such as methyl, **10c**, and methoxy, **10d**, allowed more trends to be observed between inhibitor size and affinity. It is assumed in the following discussion that the water molecule H_2O_{1S1} is always displaced by the groups larger than chlorine on the basis of the finding that chlorine displaces the water molecule in uPA, which has a large S1 subsite compared to the other proteases. The van der Waals volume of H-F, H-Cl, H-OH, H-OMe, and H-Me was calculated [using the software MOE 2000.02 from Chemical Computing Group, Inc.] and compared to that of hydrogen H-H (Table 1) to estimate the relative increase in inhibitor size in the region of residue 190 within S1. In general, a clear trend of reduced affinity with increasing

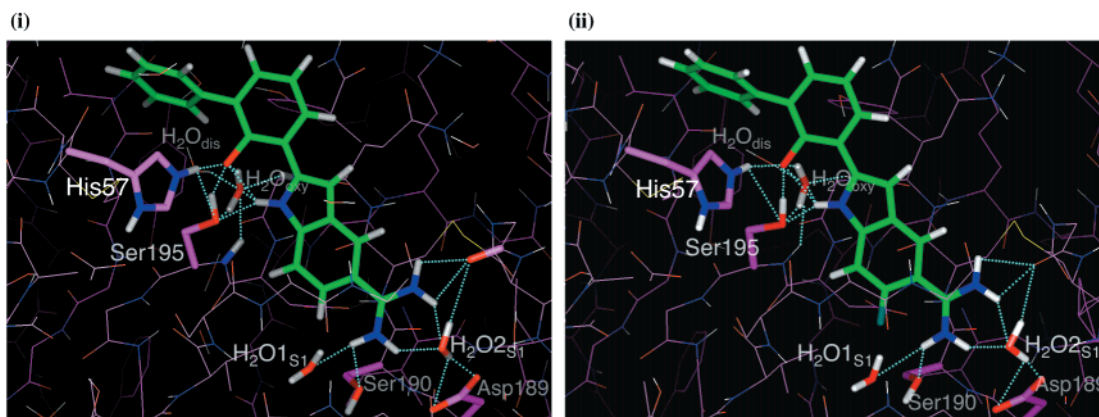


Figure 7. uPA complexes of (i) **1** and (ii) **10b**. The inhibitors have essentially the same mode of binding to uPA. The fluorine analogue **10b** does not displace H_2O_{1S1} and H_2O_{2S1} , within subsite S1. Similarly the hydrogen bond cluster involving Ser195 and His57, the inhibitor hydroxyl group, and water molecules H_2O_{oxy} and H_2O_{dis} is also unaffected by the fluorine substituent.

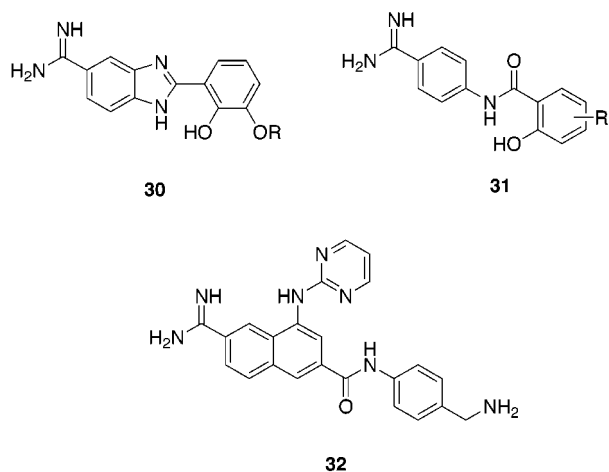


Figure 8. Alternative uPA inhibitors.

substituent size exists toward the Ser190 enzymes. This trend is not surprising on the basis of the limited space within the S1 subsite regardless of the flexibility of some of the residues. In contrast, a subtly different trend can be observed in affinity toward the Ala190 enzymes. From fluorine substitution through methyl substitution, a good correlation can be observed between affinity and increased size of the substituent. However, in the case of the methoxy analogue **10d**, three of the four Ala190 enzymes and possibly even the fourth have a greater affinity than the methyl analogue. This is most likely a reflection of the smaller size of the Ala190 group, compared to Ser190, which allows the S1 subsite to interact more favorably with the larger methoxy group. A consequence of the increased affinity of the methoxy analogue toward Ala190 enzymes and the corresponding decrease toward the Ser190 enzymes is that the selectivity is reduced. Therefore, for optimal selectivity the size of the substituent is also important, in addition to displacement of the water molecule H_2O_{1S1} in the Ala190 enzymes.

The hydroxyl analogue **10e** stands out as being the poorest inhibitor toward many of the enzymes despite a calculated van der Waals size between those of fluorine and chlorine. This indicates that affinity toward the target enzyme is also dependent on other subtle factors. One prior example of hydroxyl substitution adjacent to an amidine was reported by Choi-Sledeski et al.¹⁷ and resulted in a 21-fold drop in potency toward factor Xa. There are several potential effects that 6-position substitutions can have on the binding of the inhibitor toward a particular enzyme. The nature of the substituent and the close proximity to the amidine group generate different desolvation effects upon binding. The hydroxyl analogue is presumed to be highly solvated in solution²³ and therefore experiences a large desolvation effect when placed in the relatively nonpolar S1 subsite. The crystallographic data of the **10a** complexes also indicate that the dihedral angle between the amidine and the indole ring changes upon 6-substitution due to steric factors. In the uPA-**1** complex the amidine dihedral angle is -18° , but this changes to $+32^\circ$ in the uPA-**10a** complex. In the thrombin-**10a** complex the amidine is coplanar, experiencing steric strain which is offset by the formation of a hydrogen bond from the chlorine to the nitrogen proton.³² Finally, it is also expected that the pK_a of the amidine group, and

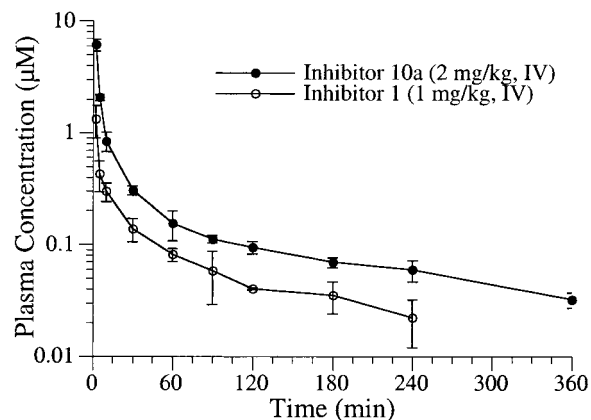


Figure 9. Plasma concentration vs time curve for **1** and **10a** following intravenous administration in male Sprague-Dawley rats.

potentially the phenol group, will change due to the different electronegative effects exerted by each different substituent. Despite these factors, it is apparent that relatively small, nonpolar groups, e.g., fluorine and chlorine, possess the appropriate characteristics for maintaining optimal potency toward the Ser190 enzymes while simultaneously displacing H_2O_{1S1} in the Ala190 enzymes to generate selectivity.

General Application to the Design of Selective Protease Inhibitors. Two of the most highly researched Ser190 enzyme targets for drug intervention are uPA and factor VIIa. Since it was clear that the fluorine and chlorine analogues held the most promise toward distinguishing between Ser190 and Ala190 proteases such as uPA/tPA and factor VIIa/factor Xa, these groups were translated onto other amidine-based inhibitors of uPA (Figure 8) and factor VIIa [unpublished results]. The 5-amidinobenzimidazole-based uPA inhibitor **30** was found to be amenable to introduction of a chlorine or fluorine atom and has yielded another class of highly potent and selective uPA inhibitors.³² Introduction of a fluorine or chlorine atom onto a benzamidine class of uPA inhibitors based upon **31** was met with limited success (Figure 8).³² Although selectivity was generated, a reduction in potency toward uPA masked much of the effect. Naphthamidine-based uPA inhibitors have also been considered as candidates for selectivity enhancement. For instance, the recently reported inhibitor **32**³³ (Figure 8) has good overall selectivity against several enzymes but in our hands has limited selectivity against the Ala190 protease p-kallikrein. Modeling of the 7-fluorine analogue of **32** in uPA indicates that this would probably displace H_2O_{1S1} and lead to an inhibitor with improved selectivity.

In Vivo Properties of 10a Compared to 1. The pharmacokinetic profiles of **1** and **10a** were measured in Sprague-Dawley rats following intravenous administration to assess the effects on clearance by the halogen substitution. The plasma concentration-time curves are shown in Figure 9, and the pharmacokinetic parameters are summarized in Table 4. The addition of the chlorine atom favorably altered the pharmacokinetic parameters and allowed plasma concentrations well above the K_i to be attained for periods of greater than 6 h, even with low doses of compound. Inhibitor **1** was eliminated from plasma in a biphasic fashion with a clearance of 121 (mL/min)/kg and a terminal half-life

Table 4. Pharmacokinetics of **1** and **10a** Following Intravenous Administration in Male Sprague-Dawley Rats

PK parameter ^a	1	10a	PK parameter ^a	1	10a
<i>n</i> ^b	3	3	<i>V</i> _c ^d (mL/kg)	1560 ± 1190	346 ± 81
dosing route	IV	IV	<i>V</i> _{ss} ^e (mL/kg)	11900 ± 3200	7700 ± 950
dose (mg/kg)	1	2	MRT ^f (min)	106 ± 49	130 ± 14
body weight (g)	286 ± 12	294 ± 7	AUC ^g (mM·min)	24 ± 8	85 ± 2
CL _p ^c (mL/min/kg)	121 ± 40	59 ± 1	<i>t</i> _{1/2} ^h (min)	102 ± 41	189 ± 32

^a PK parameters = mean ± SD values from three rats. ^b *n* = number of animals. ^c CL_p = plasma clearance. ^d *V*_c = volume of distribution in the central compartment. ^e *V*_{ss} = volume of distribution at steady state. ^f MRT = mean residence time. ^g AUC = integrated area under the plasma concentration vs time curve from time 0 to infinity. ^h *t*_{1/2} = terminal half-life.

of 102 min, whereas the modified inhibitor **10a** was cleared from plasma more slowly in a triphasic fashion, with a clearance of 59 (mL/min)/kg and a terminal half-life of 189 min. In both cases the predominant metabolite that was detected in the plasma was the glucuronide. It is thought that these pharmacokinetic parameters are sufficient to address the therapeutic potential of a uPA inhibitor in a variety of tumor models, especially on a twice daily dosing regimen. These studies are ongoing and will be reported in due course.

Conclusion

In recent years much effort has been made to generate novel S1 binding groups for trypsin-like serine proteases with the main goal of increasing oral bioavailability. Relatively little attention has been paid to this particular subsite for selectivity optimization, yet this study reveals that manipulation of the S1 binding group can also afford excellent selectivities toward subfamilies of serine proteases. Structure-based design has led to the discovery that a halogen atom insertion adjacent to the amidine of a potent and generic 5-amidinoindole-based protease inhibitor generates remarkable selectivity toward Ser190 proteases and against Ala190 proteases without substantially increasing the molecular weight. This single-atom chemical modification has transformed a potent nonselective inhibitor of uPA and tPA into a highly potent and selective inhibitor of uPA. The application of this novel and powerful method for enhancing selectivity is expected to accelerate the discovery of more potent and selective inhibitors of uPA, factor VIIa, and novel Ser190 proteases uncovered by the human genome sequencing.

Experimental Section

Reactions were carried out under an inert atmosphere at room temperature unless indicated otherwise. Solvents and chemicals were reagent grade or better. All reagents were obtained from commercial sources unless otherwise indicated. Silica gel chromatography was performed using Merck Kieselgel 60 (230–400 mesh). Preparative HPLC purification was carried out on a Gilson HPLC fitted with a VYDAC C18 (5 × 25 cm) column eluting at 50 mL/min with a gradient of 2%–90% solvent B in solvent A over 60 min (solvent A was 20 mM of aqueous HCl, and solvent B was CH₃CN). Analytical HPLC analysis was performed using an HP1100 eluting with a gradient of 2–90% solvent B in solvent A (solvent A was 0.05% TFA in water, and solvent B was CH₃CN). NMR spectroscopy was determined on a GE 300 MHz NMR or a JEOL ECLIPSE 270 MHz NMR. Chemical shifts are reported in units of δ (ppm), and peak multiplicities are expressed as follows; s, singlet; d, doublet; t, triplet; br, broad peak; q, quartet; m, multiplet; dd, doublet of doublets; ddd, doublet of doublets of doublets. Mass spectra were determined on a Perkin-Elmer Sciex API-150EX mass spectrometer equipped with a turbo ion spray source (MS-Sciex) or a Finnigan TSQ7000 equipped with an electrospray ionization source (MS-ESI). The analyti-

cal microanalyses were carried out by Robertson Microlit Laboratories Inc., Madison, NJ, and were within 0.4 unit of the theoretical values unless otherwise indicated.

2-Chloro-4-hydrazinobenzamidine (7). Ammonium chloride (7.5 g, 140 mmol) was added to *p*-xylene (100 mL) and the mixture cooled to 0 °C using an ice bath. A 2 M solution of trimethylaluminum in toluene (70 mL, 140 mmol) was added dropwise. The mixture was stirred at 0 °C for 30 min and then allowed to warm to room temperature. The nitrile **5** (8.0 g, 52 mmol) was added portionwise to the solution and the mixture refluxed for 24 h before being allowed to cool. The mixture was poured onto a slurry of silica gel (200 g) and CHCl₃ (200 mL), and then the silica gel was removed by filtration. The silica gel was washed with 50% MeOH/CHCl₃, and the combined organic solutions were then concentrated under reduced pressure. A sample was subjected to preparative HPLC chromatography to give **6** as a pale yellow solid. ¹H NMR (DMSO-*d*₆): δ 9.10 (br s, 3H), 7.26 (dd, *J* = 8.7, 2.0 Hz, 1H), 6.74 (d, *J* = 2.0 Hz, 1H), 6.62 (d, *J* = 8.7 Hz, 1H). MS-ESI: *m/z* 170 [³⁵Cl, MH⁺]. The crude product **6** was added to 6 N HCl (50 mL) and cooled to 0 °C using an ice/salt bath. A solution of NaNO₂ (4.2 g, 61 mmol) in water (15 mL) was added dropwise over 10 min. The mixture was stirred for 20 min and then added to a solution of tin(II) chloride dihydrate (16.6 g, 74 mmol) in 6 N HCl (25 mL) at –5 °C. The mixture was stirred for 30 min and then concentrated under reduced pressure to give a crude residue. Water was added and the solution concentrated under reduced pressure. The crude hydrazine product **7** was used in subsequent reactions without further purification.

6-Chloro-2-(2-hydroxybiphenyl-3-yl)-1H-indole-5-carboxamidinium (10a) and 4-Chloro-2-(2-hydroxybiphenyl-3-yl)-1H-indole-5-carboxamidinium (11). The crude hydrazine **7** (2.0 g) was added to a solution of acetophenone **8**¹ (0.48 g, 2.26 mmol) in EtOH (20 mL) followed by the addition of triethylamine (3.6 mL, 26 mmol). The solution was refluxed for 3 h and then allowed to cool. A white solid formed which was removed by filtration. The eluant was concentrated under reduced pressure to give the crude hydrazone **9**. The hydrazone was heated in PPA (10 mL) at 155 °C for 24 h to give two close-running products by analytical HPLC. The solution was allowed to cool and was then treated with 6 N HCl (10 mL) and CH₃CN (10 mL). The solid that formed was removed by filtration and the solution subjected to preparative HPLC to give the title products **10a** (11 mg, <2%) and **11** (6 mg, <1%). The spectral data for **10a** are shown in the alternative synthesis shown later. Insufficient material was obtained to allow for a full structural characterization of **11** apart from mass spectrometry analysis. MS-ESI: *m/z* 361.8 [³⁵Cl, MH⁺].

4-Amino-2-chloro-5-iodobenzonitrile (12a). 4-Amino-2-chlorobenzonitrile (**5**) (50 g, 0.3 mol) and NIS (77.4 g, 0.34 mol) were combined in AcOH (350 mL), and the resultant mixture was stirred overnight. The brown solid that formed was collected by filtration, washed with hexanes, and dried to give the title product **12a** (43.5 g, 48%) as a pale brown solid. MS-Sciex: *m/z* 278.3 [³⁵Cl, MH⁺].

2-Fluoro-4-nitrobenzoic Acid (16). To a solution of 2-fluoro-1-methyl-4-nitrobenzene (**15**) (25 g, 0.16 mol) in AcOH (250 mL) was added 18 N sulfuric acid (40 mL) dropwise over 10 min. The light yellow solution was heated to 100 °C and treated over 1 h with chromium(VI) oxide (56.4 g, 0.56 mol) dissolved in water (45 mL). The temperature of the green

mixture was maintained at 100 °C for 1 h, and then the mixture was stirred at ambient temperature overnight. The green mixture was dissolved in water (1 L) and extracted with Et₂O (4 × 200 mL). The organic extracts were combined and concentrated under reduced pressure to give a yellow solid. Water (400 mL) and K₂CO₃ (25 g) were added, and the bright yellow solution was washed with Et₂O (2 × 200 mL). HCl (12 N) was added until pH 1, and the solid that formed was collected by filtration. The solid was washed with water and dried to give **16** (15.4 g, 52%) as a light yellow solid. ¹H NMR (DMSO-*d*₆): δ 8.22–8.07 (m, 3H).

2-Fluoro-4-nitrobenzonitrile (17). A solution of 2-fluoro-4-nitrobenzoic acid (**16**) (15.4 g, 83 mmol) in THF (150 mL) at 0 °C was treated with oxalyl chloride (8.1 mL, 92 mmol) and a few drops of DMF. The solution was stirred for 1 h at 0 °C and then for 2 h at ambient temperature. The mixture was concentrated under reduced pressure, and the crude solid was dried. The solid was dissolved in THF (200 mL) and cooled to 0 °C. Ammonia gas was slowly bubbled through the mixture for 30 min, and the mixture was then capped and stirred at 0 °C for 2 h. The mixture was added to saturated NaHCO₃ (200 mL) and extracted with EtOAc (2 × 200 mL). The organic layer was dried over MgSO₄, filtered, and concentrated under reduced pressure to give the benzamide (15.5 g, 100%) as a light yellow solid. ¹H NMR (DMSO-*d*₆): δ 8.21–8.05 (m, 3H), 7.91–7.83 (m, 2H). The benzamide was dissolved in THF (400 mL) and treated with triethylamine (16.6 mL, 0.12 mol) and trifluoroacetic anhydride (14 mL, 99 mmol). The solution was stirred for 16 h at ambient temperature and then added to EtOAc (400 mL). The organic solution was washed with 0.25 N HCl (300 mL), saturated NaHCO₃, and finally brine. The organic solution was then dried over MgSO₄, filtered, and concentrated under reduced pressure to give **17** (14.7 g, 55% from **15**) as a white solid. ¹H NMR: (DMSO-*d*₆) δ 8.48–8.42 (m, 1H), 8.30–8.20 (m, 2H).

4-Amino-2-fluorobenzonitrile (18). 2-Fluoro-4-nitrobenzonitrile (**17**) (4.74 g, 29 mmol) was stirred with 10% Pd/C catalyst (500 mg) in MeOH (250 mL) under hydrogen at atmospheric pressure for 8 h. The catalyst was then removed by filtration over Celite, and the eluate was concentrated under reduced pressure to give **18** (3.9 g, 100%). ¹H NMR (DMSO-*d*₆): δ 7.38 (t, *J* = 8.6 Hz, 1H), 6.52 (br s, 2H), 6.44–6.40 (m, 2H).

4-Amino-2-fluoro-5-iodobenzonitrile (12b). The aniline **18** (3.9 g, 29 mmol) was dissolved in AcOH (60 mL) and cooled by immersion in an ice bath. NIS (6.4 g, 29 mmol) was added, and the reaction mixture was stirred for 2 h at ambient temperature. The reaction mixture was then concentrated to about one-quarter of the volume, and the solid that formed was collected by filtration. The solid was washed with hexanes and dried to give **12b** (2.45 g, 33%) as a tan solid. ¹H NMR (DMSO-*d*₆): δ 8.01 (d, *J* = 7.7 Hz, 1H), 6.61–6.55 (m, 3H).

2-Methyl-4-nitrobenzonitrile (20). The aniline **19** (15.2 g, 0.1 mol) was dissolved in water (50 mL) and AcOH (50 mL). Concentrated sulfuric acid (10.7 mL, 0.2 mol) was added and the solution cooled to 0 °C using an ice bath. NaNO₂ (7.6 g, 0.11 mol) dissolved in water (20 mL) was added dropwise over 5 min to give a mixture containing the diazonium salt. In a separate flask, copper sulfate hydrate (30 g, 0.12 mol) in water (100 mL) was cooled to 0 °C and then treated with KCN (32.5 g, 0.5 mol) in water (100 mL) over 10 min. NaHCO₃ (84 g, 1.0 mol) and benzene (100 mL) were then added to this solution followed by the diazonium mixture over 60 min. After the resultant mixture was stirred for 30 min, EtOAc was added (500 mL) and the organic layer was separated. The organic layer was washed with saturated NaHCO₃ and then dried over Na₂SO₄. The organic solution was filtered and concentrated under reduced pressure. The residual solid was resuspended in petroleum ether and collected by filtration. The solid was dried to yield **20** (14.6 g, 91%). ¹H NMR (CDCl₃): δ 8.18 (d, *J* = 0.7 Hz, 1H), 8.13 (d, *J* = 8.4 Hz, 1H), 7.79 (d, *J* = 8.4 Hz, 1H), 2.67 (s, 3H).

4-Amino-5-iodo-2-methylbenzonitrile (12c). The nitrobenzene **20** (5 g, 30 mmol) was dissolved in dioxane (27 mL),

and 12 N HCl (3 mL) was added followed by tin(II) chloride dihydrate (20.9 g, 90 mmol). The mixture was stirred for 4 h, and then EtOAc was added (50 mL). The organic layer was washed with water (100 mL). The aqueous layer was then extracted with EtOAc (2 × 50 mL). The combined organic extracts were washed with Na₂CO₃ solution and then dried over Na₂SO₄. The organic solution was filtered and concentrated under reduced pressure to give **21** (5.0 g) as a crude solid. The crude solid was dissolved in AcOH (50 mL) and treated with NIS (8.5 g, 38 mmol). The mixture was stirred for 3 h, then diluted with EtOAc (300 mL), and washed with sodium thiosulfate solution (3 × 150 mL) and then 1 N NaOH solution. The organic solution was dried over Na₂SO₄, filtered, and concentrated under reduced pressure. The residue was subjected to chromatography over silica gel eluting with 20% EtOAc in hexanes to give the title product **12c** (4.1 g, 53% from **20**). ¹H NMR (CDCl₃): δ 7.79 (s, 1H), 6.56 (s, 1H), 4.50 (br s, 2H), 2.37 (s, 3H).

2-Hydroxy-4-nitrobenzonitrile (23). 1,2-(Methylenedioxy)-4-nitrobenzene (**22**) (10.0 g, 60 mmol) was dissolved in HMPA (50 mL) and heated to 150 °C. The stirred solution was treated with NaCN (4.4 g, 90 mmol) over 20 min and then heated at 150 °C for a further 30 min. The solution was allowed to cool and diluted with water and 1 N NaOH until pH 10. The solution was washed with Et₂O (2 × 200 mL). The aqueous layer was treated with 1 N HCl until pH 6 and then extracted with EtOAc (2 × 200 mL). The organic extracts were washed with saturated NaHCO₃ and brine, dried over Na₂SO₄, filtered, and concentrated under reduced pressure. The residual solid was subjected to chromatography over silica gel eluting with 30% EtOAc in hexanes to give the title product **23** (3.0 g, 31%). ¹H NMR (DMSO-*d*₆): δ 7.98–7.94 (m, 1H), 7.75–7.71 (m, 2H). MS-Sciex: *m/z* 162.8 [*M* – H⁺].

2-Methoxy-4-nitrobenzonitrile (24). The phenol **23** (3.0 g, 18 mmol) was dissolved in anhydrous DMF (50 mL) and treated with K₂CO₃ (5.0 g, 36 mmol) followed by MeI (1.4 mL, 22 mmol). The solution was stirred for 2 h and then diluted with EtOAc (100 mL). The solution was washed with water (100 mL) and then brine, dried over Na₂SO₄, filtered, and concentrated under reduced pressure to give **24** (2.9 g, 89%). ¹H NMR (CDCl₃): δ 7.88 (dd, *J* = 8.3, 2.1 Hz, 1H), 7.82 (d, *J* = 2.0 Hz, 1H), 7.75 (dd, *J* = 8.4, 0.5 Hz, 1H), 4.05 (s, 3H).

4-Amino-5-iodo-2-methoxybenzonitrile (12d). The nitroarene **24** (2.9 g, 16 mmol) was dissolved in dioxane (45 mL) and 6 N HCl (5 mL). The stirred solution was cooled to 0 °C and treated with tin(II) chloride dihydrate (9.2 g, 49 mmol). The mixture was stirred for 3 h, allowed to warm to room temperature, and then diluted with EtOAc (150 mL). The mixture was washed with water (3 × 100 mL) and brine, dried over Na₂SO₄, filtered, and concentrated under reduced pressure to give **25** (1.8 g, 75%) as a crude solid. The solid was dissolved in AcOH (30 mL) and treated with NIS (2.7 g, 12 mmol). The mixture was stirred for 2 h and then diluted with EtOAc (200 mL). The solution was washed with water and brine, dried over Na₂SO₄, filtered, and concentrated under reduced pressure to give a crude residue. The residue was subjected to chromatography over silica gel eluting with 30% EtOAc in hexanes to give the product **12d** (1.3 g, 29% from **24**). ¹H NMR (DMSO-*d*₆): δ 7.77 (s, 1H), 6.44 (s, 1H), 6.20 (br s, 2H), 3.77 (s, 3H).

2-(Benzyloxy)-4-nitrobenzonitrile (26). The phenol **23** (2.0 g, 12 mmol) was dissolved in anhydrous DMF (30 mL) and treated with K₂CO₃ (3.3 g, 24 mmol) followed by benzyloxy bromide (1.6 mL, 13 mmol). The solution was stirred for 2 h and then diluted with EtOAc (100 mL). The solution was washed with brine (3×), dried over Na₂SO₄, filtered, and concentrated under reduced pressure to give **26** (2.2 g, 72%). ¹H NMR (DMSO-*d*₆): δ 8.11 (m, 2H), 7.93 (ddd, *J* = 8.4, 2.0, 1.0 Hz, 1H), 7.52–7.35 (m, 5H), 5.45 (s, 2H).

4-Amino-2-(benzyloxy)benzonitrile (27). The nitroarene **26** (2.7 g, 10.7 mmol) was dissolved in dioxane (20 mL) and treated with tin(II) chloride (6.1 g, 32 mmol) and 6 N HCl (2 mL). The mixture was stirred overnight and then diluted with EtOAc (100 mL). The solution was washed with 1 N NaOH,

water, and brine. The organic solution was dried over Na₂SO₄, filtered, and concentrated under reduced pressure to give **27** (2.4 g, 100%). ¹H NMR (CDCl₃): δ 7.44–7.28 (m, 6H), 6.21 (dd, *J* = 8.2, 2.0 Hz, 1H), 6.18 (dd, *J* = 7.6, 2.0 Hz, 1H), 5.12 (s, 2H). MS-Sciex: *m/z* 225.0 [MH⁺].

4-Amino-5-iodo-2-(benzyloxy)benzonitrile (12e). The amine **27** (2.4 g, 10.7 mmol) was dissolved in CH₃CN (25 mL) and treated with NIS (2.4 g, 10.7 mmol). The mixture was stirred for 2 h, and then another portion of NIS (0.48 g, 2.1 mmol) was added. The mixture was stirred overnight and then diluted with EtOAc (50 mL). The organic solution was washed with brine, dried over Na₂SO₄, filtered, and concentrated under reduced pressure. The residue was subjected to chromatography over silica gel eluting with 30% EtOAc in hexanes to give **12e** (3.0 g, 80%). ¹H NMR (DMSO-*d*₆): δ 7.80 (s, 1H), 7.46–7.32 (m, 5H), 6.54 (s, 1H), 6.20 (br s, 2H), 5.12 (s, 2H). MS-Sciex: *m/z* 351.0 [MH⁺].

N-(5-Chloro-4-cyano-2-iodophenyl)methanesulfonamide (28a). The amine **12a** (5.6 g, 20 mmol) was dissolved in CH₂Cl₂ (100 mL) and treated with *N,N*-diisopropylethylamine (DIEA) (17.4 mL, 100 mmol) and *N,N*-(dimethylamino)pyridine (DMAP) (0.25 g, 2 mmol) at 0 °C. Mesyl chloride (4.6 mL, 60 mmol) was added slowly over 15 min and the mixture stirred for 1.5 h. A further portion of DIEA (20 mL, 100 mmol) and mesyl chloride (3.0 mL, 39 mmol) were added, and the solution was stirred overnight. The mixture was concentrated under reduced pressure and the residue dissolved in EtOAc (200 mL). The organic solution was extracted with 1 N NaOH (5 × 200 mL), and the combined aqueous extracts were then acidified with 12 N HCl until pH 2. The aqueous solution was then extracted with EtOAc (3 × 500 mL), and the combined organic extracts were dried over Na₂SO₄. The mixture was filtered and the eluant concentrated under reduced pressure to give a crude residue. The residue was suspended in Et₂O and collected by filtration to give the title product **28a** (3.4 g, 47%). ¹H NMR (CDCl₃): δ 8.05 (s, 1H), 7.76 (s, 1H), 6.97 (br s, 1H), 3.13 (s, 3H).

(4-Cyano-2-fluoro-5-methoxyphenyl)carbamic Acid tert-Butyl Ester (28b). 4-Amino-2-fluoro-5-iodobenzonitrile (**12b**) (5.0 g, 19.1 mmol) and DMAP (233 mg, 1.91 mmol) were dissolved in THF (50 mL). A solution of di-*tert*-butyl dicarbonate (9.16 g, 42.0 mmol) in THF (10 mL) was added followed by DIEA (13.3 mL, 76 mmol). The mixture was stirred for 3 h, and then the solvent was removed under reduced pressure. The residue was dissolved in 1:1 THF/EtOH (40 mL). NaOH (50%) (2.53 mL, 31.3 mmol) was added and the mixture stirred for 2 h. The solvent was removed under reduced pressure and the residue dissolved in EtOAc (250 mL). The solution was washed with water (3 × 100 mL) and then brine (100 mL), dried over Na₂SO₄, filtered, and concentrated under reduced pressure. The resultant light brown residue was subjected to silica gel chromatography eluting with an increasing gradient of 10–40% EtOAc in hexanes to give **28b** (3.27 g, 47%) as a white solid. ¹H NMR (DMSO-*d*₆): δ 8.55 (s, 1H), 8.39 (d, *J* = 8.3 Hz, 1H), 7.73 (d, *J* = 13.2 Hz, 1H), 1.47 (s, 1H).

N-(5-Methyl-4-cyano-2-iodophenyl)methanesulfonamide (28c). **28c** was prepared from amine **12c** in 64% yield using the procedure described for the preparation of **28a**. ¹H NMR (CDCl₃): δ 7.99 (s, 1H), 7.59 (s, 1H), 6.88 (br s, 1H), 3.08 (s, 3H).

(4-Cyano-2-iodo-5-methoxyphenyl)carbamic Acid tert-Butyl Ester (28d). **28d** was prepared from aniline **12d** in 42% yield (with DMF as solvent) using the procedure described for the preparation of **28b**. ¹H NMR (CDCl₃): δ 8.01 (s, 1H), 7.83 (s, 1H), 7.06 (br s, 1H), 3.93 (s, 3H), 1.54 (s, 9H).

(4-Cyano-2-iodo-5-benzyloxyphenyl)carbamic Acid tert-Butyl Ester (28e). **28e** was prepared from aniline **12e** in 60% yield (with DMF as solvent) using the procedure described for the preparation of **28b**. ¹H NMR (CDCl₃): δ 8.12 (s, 1H), 7.84 (s, 1H), 7.48 (dd, *J* = 8.4, 1.8 Hz, 2H), 7.41–7.31 (m, 3H), 7.04 (br s, 1H), 5.20 (s, 2H), 1.53 (s, 9H). MS-Sciex: *m/z* 450.8 [MH⁺].

Method A: Example, 2-[2-[(2-Methoxyethoxy)methoxy]biphenyl-3-yl]-6-methyl-1*H*-indole-5-carbonitrile (29c).

The mesylate **28c** (672 mg, 2.0 mmol) was dissolved in dry DMF (20 mL). Triethylamine (2.8 mL, 20 mmol) was added followed by dichlorobis(triphenylphosphine)palladium(II) (140 mg, 0.2 mmol). The mixture was then treated with alkyne **13**¹ (564 mg, 2.0 mmol). The resultant mixture was stirred for 30 min, and then CuI (76 mg, 0.4 mmol) was added. The mixture was stirred overnight, then diluted with EtOAc (100 mL), and washed with brine (4 × 100 mL). The organic solution was dried over Na₂SO₄, filtered, and concentrated under reduced pressure. The residue was subjected to chromatography over silica gel eluting with 25% EtOAc in hexanes to give the mesylated indole (300 mg, 31%). ¹H NMR (CDCl₃): δ 7.96 (d, *J* = 0.7 Hz, 1H), 7.87 (s, 1H), 7.55–7.51 (m, 2H), 7.46–7.24 (m, 6H), 6.65 (d, *J* = 0.7 Hz, 1H), 4.51 (s, 2H), 3.35 (s, 3H), 3.11 (s, 3H), 2.98–2.86 (br m, 4H), 2.69 (s, 3H). The mesylated indole (0.30 g, 0.86 mmol) was dissolved in dioxane (10 mL), and MeOH (10 mL) and then treated with 1 N NaOH until pH 13. The mixture was stirred for 3 h and then diluted with EtOAc (100 mL). The solution was washed with brine, dried over Na₂SO₄, filtered, and concentrated under reduced pressure. The crude residue was subjected to chromatography over silica gel eluting with 25% EtOAc in hexanes to give **29c** (0.21 g, 26%). ¹H NMR (CDCl₃): δ 10.18 (br s, 1H), 7.91 (s, 1H), 7.72 (dd, *J* = 7.4, 2.2 Hz, 1H), 7.57–7.54 (m, 2H), 7.47–7.24 (m, 7H), 6.85 (d, *J* = 2.1, 0.8 Hz, 1H), 4.66 (s, 2H), 3.29–3.26 (m, 2H), 3.21–3.17 (m, 5H), 2.62 (s, 3H). MS-Sciex: *m/z* 411.0 [M – H⁺].

Method B: Example, 6-Methoxy-2-[2-[(2-methoxyethoxy)methoxy]biphenyl-3-yl]-1*H*-indole-5-carbonitrile (29d). The alkyne **13** (377 mg, 1.33 mmol) and aryl halide **29d** (500 mg, 1.33 mmol) were dissolved in dry DMF (20 mL). Triethylamine (0.93 mL, 6.65 mmol) was added followed by dichlorobis(triphenylphosphine)palladium(II) (93 mg, 0.13 mmol) and the resultant solution stirred for 30 min. CuI (51 mg, 0.27 mmol) was added and the reaction mixture stirred for a further 2 h. The mixture was diluted with EtOAc (100 mL) and washed with brine (4 × 100 mL). The organic solution was dried over Na₂SO₄, filtered, and concentrated under reduced pressure. The residue was subjected to chromatography over silica gel eluting with 20% EtOAc in hexanes to give the coupled alkyne (0.55 g, 79%). ¹H NMR (CDCl₃): δ 8.06 (s, 1H), 7.93 (s, 1H), 7.62 (s, 1H), 7.55–7.33 (m, 7H), 7.19 (t, *J* = 7.8 Hz, 1H), 4.96 (s, 2H), 3.98 (s, 3H), 3.35–3.32 (m, 2H), 3.18 (s, 3H), 3.16–3.12 (m, 2H), 1.55 (s, 9H). The coupled alkyne was then dissolved in THF (25 mL) and treated with a 1 N solution of tetrabutylammonium fluoride in THF (2.1 mL, 2.1 mmol). The mixture was refluxed for 5 h, allowed to cool, and then diluted with EtOAc (150 mL). The solution was washed with brine, dried over Na₂SO₄, filtered, and concentrated under reduced pressure. The crude residue was subjected to chromatography over silica gel eluting with 40% EtOAc in hexanes to give **29d** (395 mg, 69%). ¹H NMR (CDCl₃): δ 10.20 (br s, 1H), 7.83 (s, 1H), 7.71 (dd, *J* = 7.2, 2.5 Hz, 1H), 7.57–7.54 (m, 2H), 7.48–7.36 (m, 3H), 7.32–7.23 (m, 3H), 6.94 (s, 1H), 6.81 (dd, *J* = 2.1, 0.7 Hz, 1H), 4.67 (s, 2H), 3.94 (s, 3H), 3.37–3.33 (m, 2H), 3.28–3.25 (m, 2H), 3.23 (s, 3H). MS-Sciex: *m/z* 428.8 [MH⁺].

6-Chloro-2-[2-[(2-methoxyethoxy)methoxy]biphenyl-3-yl]-1*H*-indole-5-carbonitrile (29a). **29a** was prepared in a yield of 52% according to method A from **28a** and alkyne **13**. MS-Sciex: *m/z* 433.4 [³⁵Cl, MH⁺].

6-Fluoro-2-[2-[(2-methoxyethoxy)methoxy]biphenyl-3-yl]-1*H*-indole-5-carbonitrile (29b). **29b** was prepared in a yield of 44% according to method B from **28b** and alkyne **13**. ¹H NMR (DMSO-*d*₆): δ 8.13 (d, *J* = 6.5 Hz, 1H), 7.72 (dd, *J* = 6.5, 2.6 Hz, 1H), 7.58–7.55 (m, 2H), 7.50–7.32 (m, 7H), 7.02 (d, *J* = 1.5 Hz, 1H), 4.51 (s, 2H), 2.96–2.94 (m, 5H), 2.89–2.86 (m, 2H). MS-Sciex: *m/z* 415.1 [M – H⁺].

6-(Benzyloxy)-2-[2-[(2-methoxyethoxy)methoxy]biphenyl-3-yl]-1*H*-indole-5-carbonitrile (29e). **29e** was prepared in a yield of 54% according to method B from **28e** and alkyne **13**. ¹H NMR (CDCl₃): δ 10.16 (br s, 1H), 7.85 (s, 1H), 7.69 (dd, *J* = 7.2, 2.2 Hz, 1H), 7.56–7.23 (m, 13H), 6.97 (s, 1H), 6.80 (dd, *J* = 2.1, 0.9 Hz, 1H), 5.23 (s, 2H), 4.66 (s, 2H), 3.34–3.30 (m, 2H), 3.25–3.21 (m, 2H), 3.20 (s, 3H).

Method C: Example, 2-(2-Hydroxybiphenyl-3-yl)-6-methoxy-1*H*-indole-5-carboxamide (10d). The indole **29d** (0.39 g, 0.91 mmol) was dissolved in absolute EtOH (20 mL) and excess 50% aqueous hydroxylamine (5 mL). The mixture was refluxed for 4 h and then concentrated under reduced pressure. The crude solid was dissolved in EtOAc (50 mL) and washed with water followed by brine. The organic solution was dried over Na₂SO₄, filtered, and concentrated under reduced pressure. The crude residue containing the hydroxyamide was dissolved in AcOH (10 mL) and treated with acetic anhydride (95 μL, 1 mmol). The mixture was stirred for 1 h, and then zinc dust (~250 mg) was added. The mixture was stirred for another 4 h, and then the zinc dust was removed by filtration. The organic solution was concentrated under reduced pressure, and the crude residue containing the amidine was then dissolved in MeOH (15 mL). The solution was treated with 4 N HCl in dioxane (10 mL) and stirred for 2 h. The reaction mixture was diluted with EtOAc (100 mL) and washed with brine. The organic solution was dried over Na₂SO₄, filtered, and concentrated under reduced pressure. The crude residue was subjected to preparative HPLC to give **10d** (0.19 g, 58%). ¹H NMR (DMSO-*d*₆): δ 11.57 (s, 1H), 8.97 (br s, 2H), 8.90 (s, 1H), 8.80 (br s, 2H), 7.82 (s, 1H), 7.70 (dd, *J* = 7.5, 1.6 Hz, 1H), 7.55 (m, 2H), 7.48 (t, *J* = 7.6 Hz, 2H), 7.38 (m, 1H), 7.22–7.19 (m, 2H), 7.09 (t, *J* = 7.5 Hz, 1H), 7.03 (s, 1H), 3.89 (s, 3H). ¹³C NMR (DMSO-*d*₆): δ 165.2, 153.2, 150.5, 139.6, 138.4, 136.4, 131.8, 130.0, 129.3, 128.4, 127.1, 122.1, 121.9, 121.8, 121.0, 110.5, 102.0, 94.2, 55.9. MS-Sciex: *m/z* 358.0 [MH⁺]. Anal. (C₂₂H₁₉N₃O₂·C₂H₅F₃O₂) C, H, N.

Method D: Example, 2-(2-Hydroxybiphenyl-3-yl)-6-hydroxy-1*H*-indole-5-carboxamide (10e). The indole **29e** (0.76 g, 1.5 mmol) was dissolved in dry EtOH (20 mL), and excess 50% aqueous hydroxylamine (5 mL) was added. The mixture was refluxed for 4 h and then concentrated under reduced pressure. The crude solid was dissolved in EtOAc (50 mL) and washed with water followed by brine. The organic solution was dried over Na₂SO₄, filtered, and concentrated under reduced pressure. The crude residue containing the hydroxyamide was dissolved in AcOH (10 mL) and treated with acetic anhydride (147 μL, 1.6 mmol). The mixture was stirred for 30 min, and then 10% Pd/C catalyst (~250 mg) was added followed by MeOH (10 mL). The mixture was stirred for another 4 h under hydrogen, and then the catalyst was removed by filtration over Celite. The organic solution was concentrated under reduced pressure, and the crude residue containing the amidine was then dissolved in MeOH (15 mL). The solution was treated with 4 N HCl in dioxane (10 mL) and stirred for 2 h. The reaction mixture was diluted with EtOAc (100 mL) and washed with brine. The organic solution was dried over Na₂SO₄, filtered, and concentrated under reduced pressure. The crude residue was subjected to preparative HPLC to give **10e** (0.14 g, 27%). ¹H NMR (DMSO-*d*₆): δ 11.41 (s, 1H), 10.68 (s, 1H), 8.87 (br s, 2H), 8.82 (s, 1H), 8.60 (br s, 2H), 7.88 (s, 1H), 7.65 (dd, *J* = 7.6, 1.6 Hz, 1H), 7.55–7.53 (m, 2H), 7.47 (t, *J* = 7.5 Hz, 2H), 7.38 (d, *J* = 6.9 Hz, 1H), 7.20 (dd, *J* = 7.4, 1.5 Hz, 1H), 7.12 (s, 1H), 7.07 (t, *J* = 7.7 Hz, 1H), 6.96 (s, 1H). ¹³C NMR (DMSO-*d*₆): δ 164.9, 152.3, 150.5, 140.4, 138.4, 136.3, 131.7, 129.9, 129.3, 128.3, 127.1 (2·C), 122.0, 121.6, 120.9, 107.4, 102.2, 97.5. MS-Sciex: *m/z* 344.0 [MH⁺]. Anal. (C₂₁H₁₇N₃O₂·HCl·0.25H₂O) C, H, N, O.

6-Chloro-2-(2-hydroxybiphenyl-3-yl)-1*H*-indole-5-carboxamide (10a). **10a** was prepared from indole **29a** in a yield of 20% according to method C. ¹H NMR (DMSO-*d*₆): δ 11.85 (s, 1H), 9.35 (br s, 2H), 9.14 (br s, 2H), 9.07 (s, 1H), 7.88 (s, 1H), 7.76 (dd, *J* = 8.5, 1.7 Hz, 1H), 7.69 (s, 1H), 7.58–7.37 (m, 5H), 7.26 (dd, *J* = 8.5, 1.7 Hz, 1H), 7.15 (s, 1H), 7.12 (t, *J* = 8.5 Hz, 1H). ¹³C NMR (DMSO-*d*₆): δ 167.3, 150.5, 139.4, 138.4, 138.0, 131.3, 130.6, 129.2, 128.5, 127.5, 127.4, 127.1, 122.8, 121.4, 120.7, 120.0, 119.9, 112.6, 101.1. MS-ESI: *m/z* 361.8 [³⁵Cl, MH⁺]. Anal. (C₂₁H₁₆ClN₃O₂·HCl·0.25H₂O) C, H, N, Cl.

6-Fluoro-2-(2-hydroxybiphenyl-3-yl)-1*H*-indole-5-carboxamide (10b). **10b** was prepared from indole **29b** in a yield of 20% according to method C. ¹H NMR (DMSO-*d*₆): δ

11.91 (s, 1H), 9.22 (s, 2H), 9.17 (s, 2H), 8.93 (s, 1H), 7.86 (d, *J* = 7.7 Hz, 1H), 7.68 (dd, *J* = 8.5, 1.7 Hz, 1H), 7.50–7.28 (m, 6H), 7.17 (dd, *J* = 8.3, 1.7 Hz, 1H), 7.06–7.00 (m, 2H). ¹³C NMR (DMSO-*d*₆): δ 163.5, 150.7, 138.2, 131.9, 130.5, 129.3, 128.4, 127.6, 127.2, 124.5, 121.8, 121.6, 121.1, 109.2, 108.9, 102.1, 98.7, 98.2. MS-Sciex: *m/z* 346.1 [MH⁺]. Anal. (C₂₁H₁₆FN₃O·HCl) C, H, N, F.

6-Methyl-2-(2-hydroxybiphenyl-3-yl)-1*H*-indole-5-carboxamide (10c). **10c** was prepared from indole **29c** in a yield of 9% according to method C. ¹H NMR (DMSO-*d*₆): δ 11.64 (s, 1H), 9.17 (br s, 4H), 8.90 (s, 1H), 7.74 (d, *J* = 7.5 Hz, 1H), 7.70 (s, 1H), 7.56–7.34 (m, 6H), 7.21 (d, *J* = 7.2 Hz, 1H), 7.11–7.06 (m, 2H), 2.48 (s, 3H). ¹³C NMR (DMSO-*d*₆): δ 168.2, 150.5, 138.3, 138.1, 136.8, 131.8, 130.1, 129.2, 128.3, 127.5, 127.4, 127.0, 125.8, 121.9, 121.4, 120.9, 120.5, 112.9, 101.8, 19.7. MS-Sciex: *m/z* 341.8 [MH⁺]. Anal. (C₂₂H₁₉N₃O·HCl·0.25H₂O) C, H, N.

Enzymology. Enzymes and substrates were purchased as follows: high molecular weight (HMW) uPA (American Diagnostica), tPA (Sigma), trypsin (Worthington), thrombin (Calbiochem), plasmin (Enzyme Research Labs), and factor Xa (Haematological Technologies, Inc.). The substrates for trypsin, plasmin, and thrombin (tosyl-Gly-Pro-Lys-pNA (pNA = *p*-nitroanilide)) and for factor Xa (CH₃OCO-D-CHA-Gly-Arg-pNA-AcOH, "Pefachrome Xa") were purchased from Centerchem, Inc. The substrate for HMW uPA (Glt-Gly-Arg-AMC) was from the Peptide Institute, and the substrate for tPA (CH₃-SO₂-D-HHT-Gly-Arg-pNA, "Spectrozyme tPA") was from American Diagnostica.

Enzyme Assays. uPA was assayed spectrofluorometrically, and all the others were assayed spectrophotometrically. All enzymes were assayed at ambient temperature in 50 mM Tris, 150 mM NaCl, 0.05% (v/v) Tween-20, 10% (v/v) DMSO, 0.002% antifoam, and EDTA (1 mM) at pH 7.4. The thrombin and factor Xa assays also contained 5.0 mM CaCl₂. The final concentrations of uPA, tPA, trypsin, thrombin, plasmin, and factor Xa in the respective assays were 4 (or 5), 11 (or 15), 15, 10, 6, and 4 nM. The substrate concentrations of 85 μM (uPA), 300 μM (tPA), 25 or 45 μM (trypsin), 300 μM (thrombin), 130 μM (plasmin), and 550 μM (factor Xa) were chosen on the basis of the determined *K_m* values with EDTA of 85, 500, 45, 300, 100, and 600 μM, respectively. For uPA activity, the rate of change in relative fluorescence units (RFUs) emitted at 460 nm (excitation at 355 nm) was measured immediately after addition of enzyme. For all other enzymatic activities, the rate of change in absorbance at 405 nm was measured immediately after addition of enzyme. Apparent inhibition constants, *K_i'*, were calculated from the velocity data generated at the various inhibitor concentrations using the software package BatchKi (developed and provided by Dr. Petr Kuzmic, Biokin Ltd., Madison, WI) using methodology similar to that described for tight-binding inhibitors.³⁴ BatchKi applies nonlinear regression analysis to return nominal likelihood intervals at the 65% confidence, using the logic described by Bates and Watts.³⁵ The *K_i'* values are accepted where the nominal likelihood intervals at 65% confidence vary within 0.5–1.5-fold from the *K_i'* values. These values were converted to *K_i* values by the formula *K_i* = *K_i'*/(1 + *S*/*K_m*).

Crystallization and Preparation of Protease–Inhibitor Complexes. Procedures and conditions for crystallization have been reported by Katz et al.³²

Pharmacokinetic Study. Male Sprague–Dawley rats purchased from the Charles River Laboratory, weighing approximately 280–300 g, were used in the pharmacokinetic study. Compounds were formulated as an aqueous solution in 40% PEG400/H₂O (1 mg/mL or 2 mg/mL) and administered intravenously via bolus injection into the tail vein. Blood was collected from the jugular vein in a heparinized tube at several time points up to 24 h after dosing. Plasma samples were separated by centrifugation and kept frozen at –80 °C until analysis. Plasma concentrations were determined by LC–MS/MS on a SCIEX API 300 tandem mass spectrometer equipped with an electrospray ionization source. Samples were prepared for analysis by mixing three volume equivalents of acetonitrile

and 50 μ L of internal standard solution with the plasma sample. The samples were centrifuged and the supernatant transferred to another vial for drying by heated nitrogen gas. The sample was reconstituted in 200 μ L of mobile phase (25% acetonitrile and 0.2% formic acid in water) and injected onto the LC-MS/MS system. Chromatographic separation was performed using a C18 column (Phaenomenex, 5 μ m, 2 \times 100 mm) with a flow rate of 0.4 mL/min and a linear gradient of solvent B in solvent A (solvent A was 0.2% formic acid in water, and solvent B was 0.2% formic acid in acetonitrile). Concentrations were calculated using previously established standard curves of the inhibitors, ranging from 1 to 10000 ng/mL, and the internal standard in rat plasma. The limit of quantitation was 6 ng/mL plasma.

Pharmacokinetic parameters were estimated using Win-Nonlin Version 1.5 (Pharsight Corp., California). Pharmacokinetic calculations were performed using a nominal dose and collection time.

Acknowledgment. We thank Drs. M. Venuti, J. Knolle, and R. McDowell for helpful discussions and insights. We also thank Dr. James Janc, Dr. Kesavan Radika, and Jing Wang for the K_i determinations.

References

- Verner, E.; Katz, B. A.; Spencer, J. R.; Allen, D.; Hataye, J.; Hruzewicz, W.; Hui, H. C.; Kolesnikov, A.; Li, Y.; Luong, C.; Martelli, A.; Radika, K.; Rai, R.; She, M.; Shrader, W.; Sprengeler, P. A.; Trapp, S.; Wang, J.; Young, W. B.; Mackman, R. L. Development of Serine Protease Inhibitors Displaying a Multi-centered Short (<2.3 Å) Hydrogen Bond Binding Mode: Inhibitors of Urokinase-type Plasminogen Activator and Factor Xa. *J. Med. Chem.* **2001**, *44*, 2753–2771.
- Magill, C.; Katz, B. A.; Mackman, R. L. Emerging therapeutic targets in oncology: urokinase-type plasminogen activator system. *Emerging Ther. Targets* **1999**, *3*, 109–133. Andreasen, P. A.; Kjoller, L.; Christensen, L.; Duffy, M. J. The Urokinase-type Plasminogen Activator System in Cancer Metastasis: A Review. *Int. J. Cancer* **1997**, *72*, 1–22. Rabbani, S. A.; Xing, R. H. Role of urokinase (uPA) and its receptor (uPAR) in invasion and metastasis of hormone-dependent malignancies (Review) *J. Int. Oncol.* **1998**, *12*, 911–920.
- Deadman, J. J.; Elgandy, S.; Goodwin, C. A.; Green, D.; Baban, J. A.; Patel, G.; Skordalakes, E.; Chino, N.; Claeson, G.; Kakkar, V. V.; Scully, M. F. Characterization of a Class of Peptide Boronates with Neutral P1 Side Chains as Highly Selective Inhibitors of Thrombin. *J. Med. Chem.* **1995**, *38*, 1511–1522.
- Schechter, I.; Berger, A. On the size of the active site in proteases. I. Papain. *Biochem. Biophys. Res. Commun.* **1967**, *27*, 157–162.
- Mares-Guia, M.; Shaw, E. Studies on the Active Center of Trypsin. *J. Biol. Chem.* **1965**, *240*, 1579–1585.
- Markwardt, F. Synthetic, Low Molecular Thrombin Inhibitors. A New Concept of Anticoagulants. *Haemostasis* **1974**, *3*, 185–202.
- Geratz, J. D.; Shaver, S. R.; Tidwell, R. R. Inhibitory Effect of Amidino-substituted Heterocyclic Compounds on the Amidase Activity of Plasmin and of High and Low Molecular Weight Urokinase and on Urokinase-induced Plasminogen Activation. *Thromb. Res.* **1981**, *24*, 73–83.
- Geratz, J. D.; Stevens, F. M.; Polakoski, K. L.; Parrish, R. F.; Tidwell, R. R. Amidino-Substituted Aromatic Heterocycles as Probes of the Specificity Pocket of Trypsin-Like Proteases. *Arch. Biochem. Biophys.* **1979**, *197*, 551–559.
- Walsmann, P.; Horn, H.; Landmann, H.; Markwardt, F.; Strubebecher, J.; Wagner, G. Synthetische Inhibitoren der Serineproteinasen. *Pharmazie* **1975**, *30*, 386–389.
- Loeffler, L. J.; Mar, E.-C.; Geratz, J. D.; Fox, L. B. Synthesis of Isosteres of *p*-Amidinophenylpyruvic Acid. Inhibitors of Trypsin, Thrombin and Pancreatic Kallikrein. *J. Med. Chem.* **1975**, *18*, 287–292.
- Stürzebecher, J.; Markwardt, F. Synthetische Inhibitoren der Serineproteinasen. *Pharmazie* **1978**, *33*, 599–602.
- Yang, H.; Henkin, J. Selective Inhibition of Urokinase by Substituted Phenylguanidines: Quantitative Structure–Activity Relationship Analyses. *J. Med. Chem.* **1990**, *33*, 2956–2961. Yang, H.; Henkin, J. Competitive Inhibitors of Human Urokinase. *Fibrinolysis* **1992**, *6* (Suppl. 1), 31–34.
- Katz, B. A.; Mackman, R.; Luong, C.; Radika, K.; Martelli, A.; Sprengeler, P. A.; Wang, J.; Chan, H.; Wong, L. Structural basis for selectivity of a small molecule S1-binding submicromolar inhibitor of urokinase-type plasminogen activator. *Chem. Biol.* **2000**, *7*, 299–312.
- Brandstetter, H.; Kühne, A.; Bode, W.; Huber, R.; von der Saal, W.; Wirthensohn, K.; Engh, R. A. X-Ray Structure of Active Site-Inhibited Clotting Factor Xa—Implications for Drug Design and Substrate Recognition. *J. Biol. Chem.* **1996**, *271*, 29988–29992.
- Zhao, Z.; Arniaz, D. O.; Griedel, B.; Sakata, S.; Dallas, J. L.; Whitlow, M.; Trinh, L.; Post, J.; Liang, W. A.; Morrissey, M. M.; Shaw, K. J. Design, Synthesis, and In Vitro Biological Activity of Benzimidazole Based Factor Xa Inhibitors. *Bioorg. Med. Chem. Lett.* **2000**, *10*, 963–966.
- Ewing, W. R.; Becker, M. R.; Manetta, V. E.; Davis, R. S.; Pauls, H. W.; Mason, H.; Choi-Sledeski, Y. M.; Green, D.; Cha, D.; Spada, A. P.; Cheney, D. L.; Mason, J. S.; Maignan, S.; Guilloteau, J.-P.; Brown, K.; Colussi, D.; Bentley, R.; Bostwick, J.; Kasiewski, C. J.; Morgan, S. R.; Leadley, R. J.; Dunwiddie, C. T.; Perrone, M. H.; Chu, V. Design and Structure–Activity Relationships of Potent and Selective Inhibitors of Blood Coagulation Factor Xa. *J. Med. Chem.* **1999**, *42*, 3557–3571.
- Choi-Sledeski, Y. M.; McGarry, D. G.; Green, D. M.; Mason, H. J.; Becker, M. R.; Davis, R. S.; Ewing, W. R.; Dankulich, W. P.; Manetta, V. E.; Morris, R. L.; Spada, A. P.; Cheney, D. L.; Brown, K. D.; Colussi, D. J.; Chu, V.; Heran, C. L.; Morgan, S. R.; Bentley, R. G.; Leadley, R. J.; Maignan, S.; Guilloteau, J.-P.; Dunwiddie, C. T.; Pauls, H. W. Sulfonamidopyrrolidinone Factor Xa Inhibitors: Potency and Selectivity Enhancements via P-1 and P-4 Optimization. *J. Med. Chem.* **1999**, *42*, 3572–3587.
- (a) Rai, R.; Sprengeler, P. A.; Elrod, K. C.; Young, W. B. Perspectives on Factor Xa Inhibition. *Curr. Med. Chem.* **2000**, *1*, 1–25. (b) Fevig, J. M.; Wexler, R. R. Anticoagulants: Thrombin and Factor Xa Inhibitors. *Annu. Rep. Med. Chem.* **1999**, *34*, 81–100.
- Rijken, D. C.; Groeneveld, E. Substrate Specificity of tissue-type and urokinase-type plasminogen activators. *Biochem. Biophys. Res. Commun.* **1991**, *174*, 432–438.
- Zeslowska, E.; Schweinitz, A.; Karcher, A.; Sondermann, P.; Sperl, S.; Stürzebecher, J.; Jacob, U. Crystals of the Urokinase Type Plasminogen Activator Variant β c-uPA in Complex with Small Molecule Inhibitors Opens the Way towards Structure-based Drug Design. *J. Mol. Biol.* **2000**, *301*, 465–475.
- Nienaber, V.; Wang, J.; Davidson, D.; Henkin, J. Re-engineering of Human Urokinase Provides a System for Structure-based Drug Design at High Resolution and Reveals a Novel Structural Subsite. *J. Biol. Chem.* **2000**, *275*, 7239–7248.
- Katz, B. A.; Elrod, K. C.; Luong, C.; Rice, M.; Mackman, R. L.; Sprengeler, P. A.; Spencer, J.; Hataye, J.; Janc, J.; Link, J.; Litvak, J.; Rai, R.; Rice, K.; Sideris, S.; Verner, E.; Young, W. A Novel Serine Protease Inhibition Motif Involving a Multi-Centered Short Hydrogen Bonding Network at the Active Site. *J. Mol. Biol.* **2001**, *307*, 1451–1486.
- Dunitz, J. D. The Entropic Cost of Bound Water in Crystals and Biomolecules. *Science* **1994**, *264*, 670.
- Robinson, B. *The Fischer Indole Synthesis*; John Wiley and Sons: New York, 1982.
- Wagaw, S.; Yang, B. H.; Buchwald, S. L. A Palladium-Catalyzed Strategy for the Preparation of Indoles: A Novel Entry into the Fisher Indole Synthesis. *J. Am. Chem. Soc.* **1998**, *120*, 6621–6622.
- Yasuhara, A.; Kanamori, Y.; Kaneko, M.; Numata, A.; Kondo, Y.; Sakamoto, T. Convenient synthesis of 2-substituted indoles from 2-ethynylanilines with tetrabutylammonium fluoride. *J. Chem. Soc., Perkin Trans. 1* **1999**, 529–534.
- Fagnola, M. C.; Candiani, I.; Visentin, G.; Cabri, W.; Zarini, F.; Mongelli, N.; Bedeschi, A. Solid-Phase Synthesis of Indoles Using the Palladium-Catalyzed Coupling of Alkynes with Iodoaniline Derivatives. *Tetrahedron Lett.* **1997**, *38*, 2307–2310.
- Rudisill, D. E.; Stille, J. K. Palladium-Catalyzed Synthesis of 2-Substituted Indoles. *J. Org. Chem.* **1989**, *54*, 5856–5866.
- Larock, R. C.; Yum, E. K. Synthesis of Indoles via Palladium-Catalyzed Heteroannulation of Internal Alkynes. *J. Am. Chem. Soc.* **1991**, *113*, 6689–6690.
- Yasuhara, A.; Sakamoto, T. Deprotection of *N*-sulfonyl Nitrogen-Heteroaromatics with Tetrabutylammonium Fluoride. *Tetrahedron Lett.* **1998**, *39*, 595–596.
- Imakura, Y.; Okimoto, K.; Konishi, T.; Hisazumi, M.; Yamazaki, J.; Kobayashi, S.; Yamashita, S. Regioselective Cleavage Reaction of the Aromatic Methyleneedioxy Ring. V.¹ Cleavage with Sodium Alkoxides-Alcohols, Potassium *tert*-Butoxide-Alcohols, Dimethyl Anion-Methyl Alcohol, Metallic Sodium-Alcohols and Sodium Cyanide in Dipolar Aprotic Solvents. *Chem. Pharm. Bull.* **1992**, *40*, 1691–1696.
- Katz, B. A.; Sprengeler, P. A.; Luong, C.; Verner, E.; Elrod, K.; Kirtley, M.; Janc, J.; Spencer, J.; Breitenbucher, J. G.; Hui, H. C.; McGee, D.; Allen, D.; Martelli, A.; Mackman, R. L. Engineering Inhibitors Highly Specific for the S1 sites of Ser190 Trypsin-Like Serine Protease Drug Targets. *Chem. Biol.*, in press.

- (33) Klinghofer, V.; Stewart, K.; McGonigal, T.; Smith, R.; Sarthy, A.; Nienaber, V.; Butler, C.; Dorwin, S.; Richardson, P.; Weitzberg, M.; Wendt, M.; Rockway, T.; Zhao, X.; Hulkower, K. I.; Giranda, V. L. Species Specificity of Amidine-Based Urokinase Inhibitors. *Biochem.* **2001**, *40*, 9125–9131.
- (34) Kuzmic, P.; Sideris, S.; Cregar, L. M.; Elrod, K. C.; Rice, K. D.; Janc, J. W. High-Throughput Screening of Enzyme Inhibitors:

- Automatic Determination of Tight-Binding Inhibition Constants. *Anal. Biochem.* **2000**, *281*, 62–67.
- (35) Bates, D. M.; Watts, D. W. *Nonlinear Regression and its Applications*; John Wiley and Sons: New York, 1988.

JM010244+